8

Sinornis santensis (Aves: Enantiornithes) from the Early Cretaceous of Northeastern China

PAUL C. SERENO, RAO CHENGGANG, AND LI JIANJUN

Our current understanding of the origins and early evolution of birds (Chiappe, 1995; Norell and Makovicky, 1997; Sereno, 1997, 1999b; Forster et al., 1998; Padian and Chiappe, 1998) has been strongly influenced by remarkable skeletons of basal birds and other coelurosaurs discovered recently in lacustrine deposits of Early Cretaceous age in Liaoning Province, China. The first Mesozoic avian remains reported from this region consisted of a partial skeleton of a sparrow-sized bird named *Sinornis santensis* (Sereno and Rao, 1992). *S. santensis* was discovered in a richly fossiliferous lacustrine facies of the Jiufotang Formation (Chen, 1988). Shortly after its discovery, several additional avian skeletons of similar size were discovered in the same local region and horizons and described as *Cathayornis yandica, Boluochia zhengi,* and others (Zhou et al., 1992; Zhou, 1995a,b; Hou, 1997; Zhou and Hou, Chapter 7 in this volume).

In this chapter, we provide a brief description of the skeletal anatomy of *S. santensis,* discuss its relationship with other avian remains from the same levels, and consider its phylogenetic position among early avians.

The following institutional abbreviations are used in this chapter: BVP, Beijing Natural History Museum, Paleovertebrate Collection, Beijing, China; IEI, Institut d'Estudis Illerdencs, Castile–La Mancha, Spain; IVPP, Institute of Vertebrate Paleontology and Paleoanthropology, Beijing, China; UAM, Universidad Autónoma de Madrid, Madrid, Spain.

Geological Setting

In July 1987, a young boy living in the countryside near Chaoyang city in Liaoning Province (Fig. 8.1) noticed some fossil bone on a small mudstone slab. He brought pieces of the slab to Yan Zhiyou, a local farmer known for his interest in fossils. Yan Zhiyou, in turn, reported the possible discovery of a small fossil bird to the Beijing Natural History Museum in 1988. Two of us (Li J. and Rao C.) visited Yan Zhiyou and confirmed the avian affinity of the specimen and site of discovery. The specimen underwent acid preparation, and an initial description was published (Rao and Sereno, 1990; Sereno and Rao, 1992). Additional specimens were discovered in the same area in 1990 by Zhou Zhonghe of the Institute of Vertebrate Paleontology and Paleoanthropology and described as *C. yandica* (Zhou et al., 1992; Zhou, 1995a; Zhou and Hou, Chapter 7 in this volume) and *B. zhengi* (Zhou, 1995b).

All these specimens were discovered in lacustrine facies of the Jiufotang Formation in association with the Jehol fauna, characterized by abundant remains of the teleost *Lycoptera,* the insect *Ephemeropsis,* and the conchostracan *Eosestheria* (Hong, 1988). Two species of the ornithischian dinosaur *Psittacosaurus* (*P. meileyingensis, P. mongoliensis*) are recorded in overlying nonmarine facies of the Jiufotang Formation (Sereno et al., 1988).

The Jiufotang Formation lies stratigraphically above the Yixian and Chaomidianzi Formations (Wang et al., 1998; Ji et al., 1999). The Chaomidianzi Formation, which has yielded many skeletons of *Confuciusornis sanctus* (Hou et al., 1995, 1996; Chiappe et al., 1999) and other taxa (Barrett, 2000), has recently been radiometrically dated as Barremian in age (Swisher et al., 1999), which suggests that the Jiufotang Formation may be as young as Aptian or Albian in age (100 million–120 million years old).

Systematic Paleontology

The phylogenetic definitions of taxa in the hierarchy listed subsequently and shown in Figure 8.9A are briefly reviewed.

Aves—Chiappe (1992:348) defined Aves as "the common ancestor of *Archaeopteryx* and modern birds [Neornithes] plus all its descendants." Sereno (1997:459) used *Archaeop-*

Figure 8.1. Map of Liaoning Province in northeastern China showing Shengli (type locality of *S. santensis*), Boluochi (type locality for *C. yandica*), and the Sihetun-Jianshangou region (type locality of *C. sanctus*).

teryx and Passeriformes for the same. Later, in a more formal consideration of taxa, Sereno used *Archaeopteryx* and Neornithes as reference taxa (1998:65), with Neornithes, in turn, defined as *Struthio, Passer,* their common ancestor, and all descendants (1998:59). The use of vernacular terms as reference taxa, such as "extinct birds," is best avoided for clarity (Sereno, 1999b). All these definitions, nonetheless, correspond well with the traditional taxonomic content of Aves.

Gauthier (1986:36), on the other hand, suggested that Aves be restricted to crown birds alone and defined as "the most recent common ancestor of Ratitae, Tinami, and Neognathae, and all of its descendants." This crown group definition has priority over those mentioned previously (Sereno, 1998: table 2) but excludes from Aves many extinct sister taxa that have been regarded as birds for more than a century. Substituting a new taxon, Avialae, to identify a clade long recognized as Aves (Gauthier, 1986) has not gained wide acceptance. Invoking entrenched historical usage, however, may be the only reason to set aside Gauthier's phylogenetic definition of Aves (see also Witmer, Chapter 1 in this volume; Clark, Norell, and Makovicky, Chapter 2 in this volume).

Ornithurae—Gauthier (1986:36) provided the first phylogenetic definition of Ornithurae. He coined a stem-based taxon that included "Aves [i.e., living birds] plus all extinct maniraptorans that are closer to Aves than is *Archaeopteryx.*" Cracraft (1986:385) used the same definition, stating that "*Archaeopteryx* is the sister-group of all other birds; this latter taxon is here termed the Ornithurae (following Martin 1983a [Martin 1983 in this chapter]; and Gauthier, 1986)." Sereno (1997:459) followed this definition, recognizing *Archaeopteryx* and Neornithes as formal reference taxa (1998:65).

Chiappe (1996:205), on the other hand, redefined Ornithurae as a node-based taxon including only "Hesperornithiformes and Neornithes plus all taxa descended from it." Two reasons were given: convenience and historical usage. Chiappe (1991:337) stated that Ornithurae was "defined by previous authors as a taxon including extant birds and all extinct birds that are closer to them than is *Archaeopteryx* (Cracraft, 1986; Gauthier, 1986). These authors diagnosed Ornithurae on the basis of several derived features, most of which are accepted here. However, the recent discovery of several new fossil birds which lack the synapomorphies noted earlier (e.g., the Las Hoyas bird (Sanz et al., 1988), Enantiornithes (Walker, 1981; Martin, 1983)) makes it convenient to adopt a stricter definition of Ornithurae." This reasoning is in conflict with one of the principal aims of phylogenetic taxonomy—to replace taxa based on suites of characters with node- or stem-based definitions that reduce ambiguity in taxonomic content and eliminate arbitrary definitional revisions of this kind. Traditional usage (Chiappe, 1996:205), likewise, cannot be invoked to alter the original node-based definition of Ornithurae. Historical use of Ornithurae does not correspond to that preferred by Chiappe (Sereno, 1999b), and recent use of Ornithurae, when associated with informal phylogenetic definitions (e.g., Martin, 1983; Cracraft, 1986), is consistent with Gauthier's original definition (Sereno, 1999c). The editors of this volume, nevertheless, have instructed contributing authors to adopt Chiappe's more restrictive definition for Ornithurae. To avoid confusion, the taxon Ornithurae will not be used in the text of this chapter.

Ornithothoraces—"Ornithopectae" was defined as "the common ancestor of the Las Hoyas bird and extant birds, plus all their descendants" (Chiappe, 1991:337). Chiappe and Calvo (1994: Fig. 9) and Chiappe (1996:205) substituted Ornithothoraces for "Ornithopectae" and *Iberomesornis romerali* for the "Las Hoyas bird." Sereno (1998:65) defined Ornithothoraces in a similar manner as a node-based taxon but used *S. santensis*—a more completely known member of Enantiornithines—and Neornithes as reference taxa.

Enantiornithes—Sereno (1998:65) provided a stem-based definition for Enantiornithes—"all ornithothoracines closer to *Sinornis* than to Neornithes."

Taxonomic Hierarchy

Aves Linnaeus, 1758
  Ornithothoraces Chiappe and Calvo, 1994
    Enantiornithes Walker, 1981
      Sinornis Sereno and Rao, 1992
      (= *Cathayornis* Zhou, Jin, and Zhang, 1992)

Diagnosis—See type species.

S. santensis Sereno and Rao, 1992
(= *C. yandica* Zhou, Jin, and Zhang, 1992)

Holotype—BPV 538a and 538b constitute part and counterpart, respectively, of a single articulated skeleton in the collections of the Beijing Natural History Museum. A triangle in the center of the skeleton is missing from both part and counterpart, and the smaller counterpart slab covers only the caudal one-half of the skeleton. The counterpart (BPV 538b) is preserved as discovered, with the majority of the bones exposed in cross section. The part (BPV 538a) was prepared in acid and now is preserved as a natural mold, from which an epoxy cast was made. All the descriptive detail is based on the epoxy cast derived from the part (BPV 538a), drawn with a camera lucida (Figs. 8.2–8.7).

An earlier drawing was made prior to acid preparation and was based on tracings from part and counterpart slabs (Sereno and Rao, 1992: Fig. 2). Right and left hindlimbs were misidentified, and the view chosen (right lateral) is the reverse of that now available from the epoxy cast of the part slab (left lateral) (Figs. 8.2–8.7).

Referred specimens—Referred material includes IVPP V9769A, B (holotypic specimen of *C. yandica*) and several other specimens in the collections of the IVPP from the same region (just south of Boluochi, Liaoning Province; Zhou, 1995a) (Fig. 8.1).

Synonomy—Like *S. santensis*, the holotypic specimen of *C. yandica* (IVPP V9769A, B; Zhou et al., 1992) comes from lacustrine facies in the lower portion of the Jiufotang Formation near the city of Chaoyang, Liaoning Province, in northeastern China, approximately 15 km from the type locality of *S. santensis* (Fig. 8.1; Zhou, 1995a: Fig. 1). *S. santensis* and *C. yandica* were named and described independently (the former shortly before the latter) without comparison. Now that both holotypic skeletons have undergone acid preparation, a detailed comparison is possible. The holotypic skeleton of *C. yandica* is extremely similar to that of *S. santensis*.

Cranial comparisons are limited to the maxilla and nasal. Each specimen preserves the caudal portion of the antorbital fossa and the flat external surface of the maxilla below the fossa in lateral view. Unlike *Archaeopteryx* (Elzanowski and Wellnhofer, 1996: Fig. 7), the external surface of the maxilla has parallel dorsal and ventral margins and does not taper in depth caudally until very near its articular end for the jugal. Both specimens also preserve articulated nasals in dorsal view. In contrast to *Archaeopteryx* (Elzanowski and Wellnhofer, 1996: Fig. 7), the caudal half of the nasal is more transversely expanded, flaring abruptly caudal to the external naris. In both specimens the nasal terminates caudally as a broad triangular sheet separated in the midline from its opposite by an equally broad V-shaped frontal embayment. The caudal end of the nasal and the median frontal embayment appear to be narrower in *Archaeopteryx* (Elzanowski and Wellnhofer, 1996: Fig. 7).

Comparisons of the axial column are limited to thoracic, sacral, and caudal vertebrae and the pygostyle. The vertebrae are very similar to each other and to those of other enantiornithines (Chiappe and Walker, Chapter 11 in this volume). Midthoracic vertebrae have amphicoelous, spool-shaped centra, and the cupped articular surface of the parapophysis is caudally displaced on the neural arch. There are eight sacral vertebrae, the centra of which are broad and flat ventrally and the ribs of which increase in length caudally (Zhou, 1995a: Fig. 5). The relatively short caudal centra are broader than deep and have broad, bulbous chevron facets ventrally. The pygostyle is characteristic in *C. yandica* and *S. santensis*. Unlike *Iberomesornis* (Sanz and Bonaparte, 1992; Sereno, 2000), dorsal and ventral processes flare beyond the dorsal and ventral margins of the base of the pygostyle, and the lateral crest is located at midheight along the pygostyle (Fig. 8.2). The basal processes are smaller in *Iberomesornis*, and the lateral crest is situated along the ventral margin (Sereno, 2000: Fig. 7). In *C. sanctus*, the basal processes of the pygostyle are not as pronounced as in *S. santensis* and *C. yandica*, but the lateral crest is located in a similar position at midheight along the pygostyle (Martin et al., 1998: Fig. 2E; Chiappe et al., 1999: Fig. 25).

The long bones of the postcranial skeleton are approximately 10% longer in the holotypic specimen of *C. yandica* than in *S. santensis* (Tables 8.1, 8.2). Ratios between and within the forelimb and hindlimb, however, are nearly identical and similar to those in two other enantiornithines (Table 8.3). In the forelimb, the ungual of manual digit II is larger than that of digit I in *S. santensis* (BPV 538a); in the holotypic specimen of *C. yandica*, the unguals appear to be subequal in size and length. Phalanx 1 of manual digit III curves away from digit II to a greater degree in *S. santensis* (BPV 538a), but the form of this reduced phalanx appears to be somewhat variable among ornithothoracines. Zhou (1995a: Figs. 8, 9) and Hou (1997:107) have shown metarpals II and III in contact, or fused, along their shafts, lacking the intermetacarpal space that is present in *S. santensis* and most other avians. The lack of an obvious intermetacarpal space in *C. yandica*, however, is the result of postmortem flattening of the metacarpus, which has deflected the narrow shaft of metacarpal III against the more robust shaft of metacarpal II. An intermetacarpal space is present in the right metacarpus of IVPP V9769B, as seen in ventral view.

The pelvic girdle is very similar in *S. santensis* and *C. yandica*. The ilium and pubis are identical in shape and proportions, although the dorsal margin of the ilium in *S. santensis* and the pubic foot in *C. yandica* are not preserved and

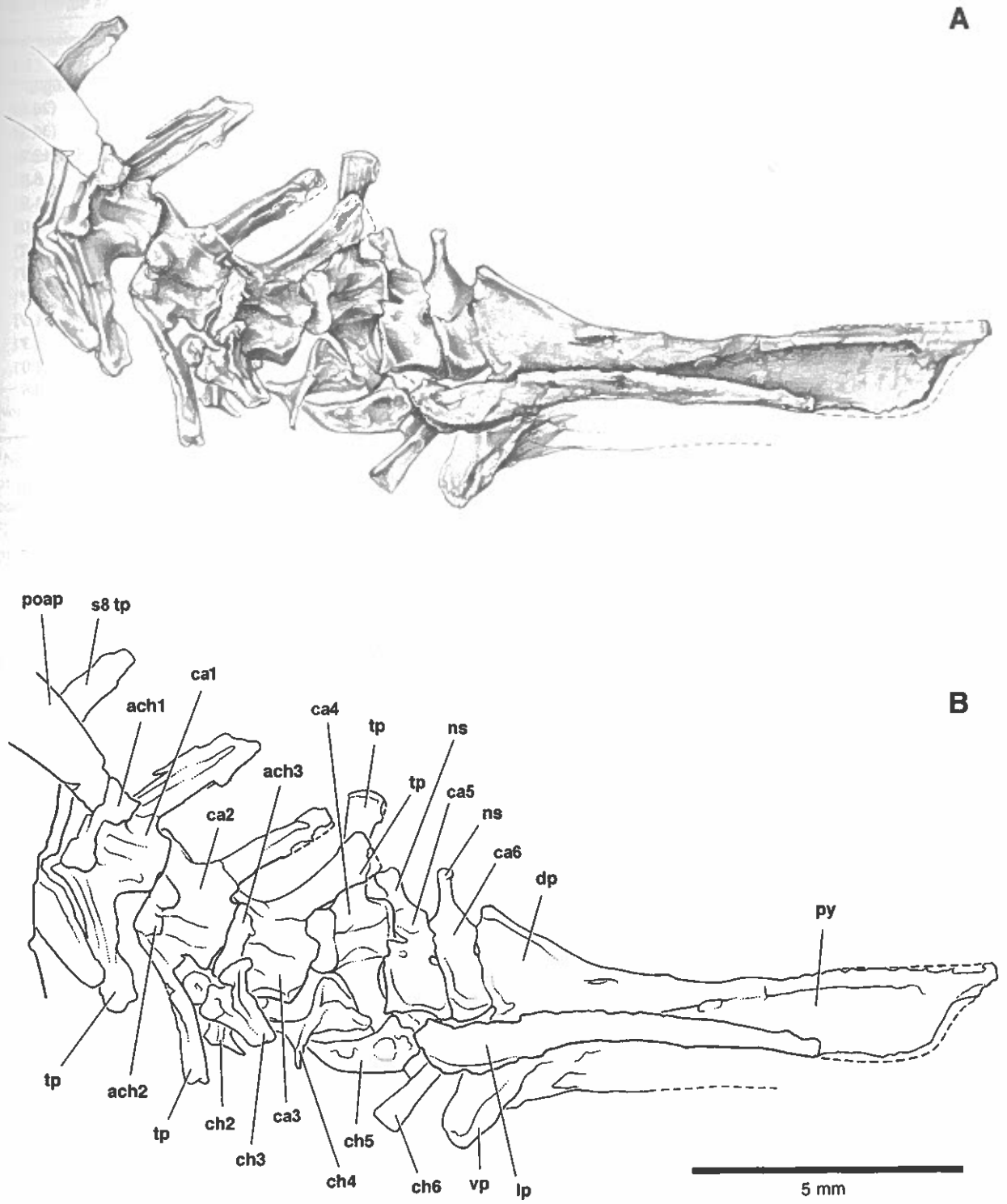

Figure 8.2. Caudal vertebrae and pygostyle of *S. santensis* (BPV 538a, epoxy cast) in left lateral view (A, B). Broken lines indicate bone margins visible as impressions. Abbreviations: ach1–3, articular surface for chevrons 1–3; ca1–6, caudal vertebrae 1–6; ch2–6, chevrons 2–6; dp, dorsal process; lp, lateral process; ns, neural spine; poap, postacetabular process; py, pygostyle; s8, eighth sacral vertebra; tp, transverse process; vp, ventral process.

cannot be compared. The elongate, scimitar-shaped ischium in *S. santensis* has an unusual reflected lamina on its lateral side, and the elongate, curving profile and lamina are exposed on the right ischium of *C. yandica* (IVPP V9769B). No differences are apparent in the hindlimb.

Although clearly very similar to each other, *S. santensis* and *C. yandica* are also very similar to *Concornis lacustris* (Sanz et al., 1995) and *I. romerali* (Sanz and Bonaparte, 1992; Sereno, 2000; Sanz et al., Chapter 9 in this volume). Ultimately, synonymy must be based on the presence of autapomorphies, of which there are only a few. In both *S. santensis* and *C. yandica,* the base of the pygostyle has prominent and flaring dorsal and ventral processes, and a lateral crest is present at midheight along the length of the pygostyle. In both of these species, the ischium has a thin lamina in its proximal half that is reflected ventrally. The ischiadic lamina and the elongate, curved shape of the blade are probably more diagnostic and less variable than pygostyle form. As these features have not been observed in other enantiornithines, *C. yandica* is regarded as a junior synonym of *S. santensis,* a synonymy acknowledged previously as a possibility by Zhou (1995a:6; see also Zhou and Hou, Chapter 7 in this volume).

The systematic status of other basal avians described recently from the same beds will remain unclear until they are described in more detail. *B. zhengi* appears to be distinct (Zhou, 1995b), but *Cathayornis caudatus* and *Longchengornis sanyanensis* (Hou, 1997: Figs. 51, 59) may eventually be regarded as junior synonyms of *S. santensis.*

Locality and horizon—Chaoyang County, Liaoning Province, People's Republic of China; lacustrine facies in the lower part of the Jiufotang Formation; Early Cretaceous (? Aptian-Albian) (Fig. 8.1; Sereno and Rao, 1992:848; Zhou, 1995a; Swisher et al., 1999).

Revised diagnosis—Sparrow-sized enantiornithine very close in form to *C. lacustris* and characterized by an elongate, scimitar-shaped ischiadic blade (narrowest width approximately one-tenth ischiadic length), a ventrally reflected lamina on the lateral aspect of the proximal half of the ischium, flaring dorsal and ventral processes at the base of the pygostyle, and a lateral crest situated at midheight along the pygostyle.

Anatomy

The following description is based primarily on an epoxy cast made from the natural mold of the part (BPV 538a) of the holotypic skeleton. The smaller counterpart was not prepared in acid. Additional information and comparisons are based on epoxy casts of the part and counterpart of a referred specimen, IVPP V9769 (*C. yandica*), also preserved as a natural mold. Epoxy casts of these two speci-

TABLE 8.1

Measurements of the holotypic skeleton of *Sinornis santensis* (BPV 538a, epoxy cast) in mm

Skull and Axial Column			
Skull length			(26.5)
Dorsal vertebral column, length			(30.5)
Sacrum length			12.9
CA1–6 length			8.4
Pygostyle length			11.5
Furcula, dorsolateral ramus, length			(8.0)
Hypocleideum length			6.0
?C12	2.4	CA1	1.6
?D1	2.4	CA2	1.5
?D8	2.3	CA3	1.5
S1	(2.5)	CA4	1.3
S8	(1.5)	CA5	1.0
		CA6	0.6
Pectoral Girdle and Forelimb			
Scapula (left)			
Length (left)			(18.0)
Width of distal blade			1.5
Humerus (right)			
Length			24.0
Ulna (left)			
Length			(19.2)
Midshaft diameter			2.0
Radius (left)			
Length			(22.2)
Midshaft diameter			1.0
Carpometacarpus			
Metacarpal I (right)			(1.9)
Metacarpal II (left)			10.3
Metacarpal III (right)			(10.8)
Manual phalanges[1] (right)			
I-1 (left)			4.0
I-ungual			1.6
II-1			5.4
II-2			3.8
II-ungual			2.1
III-1			3.9
Pelvic Girdle and Hindlimb			
Ilium (left)			
Length			(13.0)
Acetabulum, craniocaudal diameter			1.8
Femur (right, left)			
Length			(21.0)
Tibiotarsus			
Length (right)			26.4
Length (left)			25.7
Tarsometatarsus (right)			
Metatarsal I			3.2
Metatarsal II			14.1
Metatarsal III			14.6
Metatarsal IV (left)			14.1

(continued)

TABLE 8.1 *(continued)*

Pelvic Girdle and Hindlimb	
Pedal phalanges[1] (right)	
I-1	3.7
I-ungual[2]	5.6
II-1	3.2
II-2	4.1
II-ungual[2]	5.8
III-1	4.3
III-2	3.6
III-3	3.9
III-ungual[2]	6.7
IV-1	2.1
IV-2	2.1
IV-3	2.1
IV-4	3.0
IV-ungual[2]	5.3

Note: Parentheses indicate estimated measurement. Abbreviations: C, cervical; CA, caudal; D, dorsal; S, sacral.
[1]Nonungual phalangeal length is measured from the deepest part of the proximal articular cotyla to the apex of the farthest distal condyle.
[2]Pedal ungual length measured as a chord from the extensor process of the base to the tip of the ungual sheath.

mens are identified hereafter as the "holotypic" and "referred" specimens.

Skull

Dermal Skull Roof. The skull of the holotypic specimen is partially disarticulated and rotated so that the snout is pointing caudally. The premaxillary portion of the snout extends beyond the preserved edge of the slab. The nasals are flattened in the plane of the slab and are exposed in dorsal view. The orbital region of the skull is visible in right lateral view, and several sclerotic plates from the left sclerotic ring are preserved within the orbit. The caudal skull roof and occipital condyle are preserved in dorsal view. Portions of the dermal skull roof (maxilla, nasal, lacrimal), palate, occiput, and portions of the lower jaws (surangular, angular, splenial) are exposed.

The skull of the referred specimen is more articulated and is preserved in left lateral view on the part (IVPP V9769A; Zhou, 1995a: Fig. 3). Only the tip of the snout is preserved on the counterpart (IVPP V9769B). The oval external naris is large and retracted from the rostral end of the snout as in *Archaeopteryx* and nearly all other birds. The antorbital cavity is invaginated along its ventral margin as best seen in the holotypic specimen. An oval maxillary fenestra may have been present on the medial wall of the antorbital cavity; the region is best preserved in the right maxilla of the referred specimen, which is exposed in medial view. Another enantiornithine skull has been shown as lacking the

TABLE 8.2

Comparative measurements of the holotypic skeleton of *Cathayornis yandica* (IVPP V9769A, B, epoxy cast) in mm

Skull and Axial Column	
Skull length	28.2
Sacrum length	13.1
Pygostyle length	14.4
Furcula, dorsolateral ramus length	9.6
Hypocleideum length	4.5
?C9	2.7
?C10	2.5
?D4	2.7
CA1	2.0
CA5	1.6
Pectoral Girdle and Forelimb	
Scapula	
Length (right)	19.6
Width of distal blade (left)	1.3
Humerus (right)	
Length	27.0
Ulna (right)	
Length	26.4
Midshaft diameter	2.3
Radius (right)	
Length	25.3
Midshaft diameter	1.2
Carpometacarpus	
Metacarpal I (right)	2.2
Metacarpal II (left)	11.5
Metacarpal III (right)	13.0
Manual phalanges[1] (left)	
I-1 (right)	4.7
I-ungual	1.8
II-1	6.9
II-2	4.2
II-ungual	1.8
III-1 (right)	3.3
Pelvic Girdle and Hindlimb	
Ilium (left)	
Length	13.9
Femur (left)	
Length	23.1
Tibiotarsus (right)	
Length	29.0
Tarsometatarsus (right)	
Metatarsal I	3.0
Metatarsal II	14.8

Note: Abbreviations: C, cervical; CA, caudal; D, dorsal; S, sacral.
[1]Nonungual phalangeal length is measured from the deepest part of the proximal articular cotyla to the apex of the farthest distal condyle.

TABLE 8.3

Comparative ratios of long bones in the holotypic specimens of *Iberomesornis romerali*, *Concornis lacustris*, *Sinornis santensis*, and *Cathayornis yandica*

Ratios	*Iberomesornis*	*Concornis*	*Sinornis BPV 538a*	*Sinornis (= Cathayornis) IVPP V9769*
h/r	(0.97)	1.13	(1.08)	1.07
f/tt	0.82	0.69	(0.81)	0.80
tt/mtIII	1.70	1.74	1.79	(1.88)
h/f	1.06	1.31	1.14	1.17
h+r/f+tt	0.98	1.00	0.98	1.00

Source: Measurements for *Iberomesornis* and *Concornis* are from Sereno, 2000.
Note: Parentheses indicate ratios that are based on one estimated length measurement. Abbreviations: f, femur; h, humerus; mtIII, metatarsal III; r, radius; tt, tibiotarsus.

maxillary fenestra (Sanz et al., 1997), but that part of the bone is not well preserved.

The elongate caudodorsal process of the premaxilla extends to the caudal end of the external naris (Zhou, 1995a: Fig. 3) as in *Archaeopteryx*. In *Confuciusornis* and more advanced ornithurines, in contrast, this process extends farther caudally to contact the frontals (Martin et al., 1998; Chiappe et al., 1999). The external surface of the caudal ramus of the maxilla is strap-shaped with parallel dorsal and ventral margins, as preserved in the holotypic and referred specimens. Rostrally, the nasal is transversely narrow and arched. Caudally, it expands as a broad sheet, and there is a V-shaped embayment in the midline between opposing nasals. The elongate jugal is strap-shaped (transversely compressed), rather than rod-shaped, below the orbit, and it has a well-developed, caudodorsally inclined postorbital process. The slender postorbital process of the jugal is very similar to that in an enantiornithine skull from Spain (IEI LH-4450), although this process was not described in the latter (Sanz et al., 1997: Fig. 3). A postorbital may be preserved in the holotypic specimen but cannot be identified with certainty. The postorbital, however, is preserved in other enantiornithines (Sanz et al., 1997; Chiappe and Walker, Chapter 11 in this volume). The frontal and parietal form the domed caudal portion of the cranium. A portion of the occipital condyle may be exposed in the holotypic specimen.

Palate. The quadrate head is partially exposed in the holotypic specimen and appears to be developed as a single condyle. Zhou (1995a: Fig. 3) identified a quadrate in the referred skull, but we cannot confirm this identification. The area of bone in question in the referred skull is very broken. In the holotype, the right pterygoid is exposed in articulation with the basisphenoid, caudally, and ectopterygoid, laterally. The quadrate wing of the pterygoid expands caudally as a sheet.

Lower Jaw. The lower jaw is deeper caudally than rostrally. The dentary ramus, in particular, is very slender. Its pointed rostral end is slightly upturned in lateral view, as seen in the referred skull. The splenial has a broad triangular shape and is pierced by a foramen in both specimens. The left angular and prearticular are exposed in medial view in the holotypic specimen and are similar in shape to that in *Archaeopteryx* (Elzanowski and Wellnhofer, 1996).

Teeth. Preserved only in the referred specimen, the teeth are fewer in number than in *Archaeopteryx*. There are four premaxillary teeth that increase in size caudally (Zhou, 1995a). The crowns are subconical with a subtle basal constriction as in *Archaeopteryx*. One crown is preserved toward the rostral end of the left maxilla in the referred specimen. At least the caudal two-thirds of the maxilla, however, is edentulous. Similarly, the slender dentary clearly lacks teeth along most of its length. One dentary tooth, preserved on both sides in the referred specimen, projects into the gap between premaxillary and maxillary teeth.

Axial Column

Presacral Vertebrae. None of the cervicals are preserved in the holotypic specimen. A series of five midcervical vertebrae are preserved in the referred specimen, which are exposed in dorsal view (IVPP V9769A). The caudal two of these are also exposed in ventral view (IVPP V9769B). The elongate, spool-shaped centra have a low ventral keel that spans the length of the centrum. Partially exposed articular faces show some development of heterocoely; rostral surfaces are transversely concave and dorsoventrally convex, similar to that in a better exposed enantiornithine cervical series (Sanz et al., 1997). In dorsal view, the neural arches are proportionately broad, and the vertebral canal is spacious. The postzygapophyses arch dorsally, and the neural spines are low.

Best exposed in the holotypic specimen, the thoracic vertebrae have a broad, poorly defined pleurocoel. An espe-

cially robust ventral keel is present on the centrum of the most cranial thoracic vertebra. The parapophysis projects over the pleurocoel and is deeply cupped, as in other enantiornithines (Chiappe and Walker, Chapter 11 in this volume). Middorsal vertebrae have spool-shaped amphicoelous centra without ventral keels. The neural canal is large, and the flat zygapophyseal articulations are set at about 45° from the horizontal (BPV 538a). The broad neural spines are craniocaudally longer than tall and angle caudodorsally (IVPP V9769A).

Sacral Vertebrae. The sacrum consists of eight fused vertebrae, as best seen in the referred specimen, and is disarticulated from the ilium in both specimens. The cranialmost sacral, exposed in ventral view in the holotypic specimen, has a spool-shaped centrum cranially but flattens caudally. The cranial articular face is gently concave. Sacrals 1–5 have broad centra and plate-shaped transverse processes. In *Iberomesornis*, sacrals 1–3 and 6–8 are associated with pre- and postacetabular processes, respectively, and sacrals 4 and 5 attach to the ilium just above the acetabulum (Sereno, 2000). The shape of the sacral series in *Sinornis* suggests that it attached to the ilium in a similar manner. The transverse processes that attach to the postacetabular process, for example, angle backward and decrease in length and width, as is well exposed in the referred specimen (Zhou, 1995a).

Caudal Vertebrae. There are six free caudal vertebrae, as in *Iberomesornis* (Sereno, 2000; contra Sanz and Bonaparte, 1992). The number of caudal vertebrae is most easily ascertained in the holotypic specimen (Fig. 8.2), although the same number is present between the sacrum and pygostyle in the referred specimen (contra Zhou, 1995a:11–12). The transverse processes decrease in length and width and shift from a caudolateral to a lateral orientation near the pygostyle. The transverse processes are long on the fourth caudal but appear to be absent on the fifth and sixth caudal vertebrae, lateral to which projects the lateral process of the pygostyle. The form of the caudal neural arches is not well known because the proximal four caudal vertebrae are exposed in ventral view (Fig. 8.2). Neural spines are present on the fifth and sixth caudal vertebrae. Robust paired chevron facets are present, and it is noteworthy that these are located on the proximal, rather than distal, margin of the centra.

Pygostyle. As in other enantiornithines and *Confuciusornis*, the pygostyle is large, exceeding the collective length of the free caudals (Fig. 8.2). Best preserved in the holotypic specimen, the pygostyle is deepest proximally and narrowest at midlength. At its proximal end, sagittal, dorsal, and ventral processes are well developed. A strong lateral process extends proximally lateral to the sixth, and the distal half of the fifth, free caudal. The lateral process extends distally as a lateral shelf along most of the length of the pygostyle.

Ribs. The short cervical ribs are fused to the transverse processes, as preserved in the referred specimen and in other enantiornithines (Sanz et al., 1996, 1997). They extend parallel to the centra and stop short of its caudal articular surface. The first thoracic rib is transitional in form between the short cervical ribs and the broad and long cranial dorsal ribs (BPV 538a). About half the length and width of the other cranial thoracic ribs, the first thoracic rib tapers to a slender pointed distal end. The rib shafts of the second and more caudal cranial thoracic ribs are very broad and strap-shaped. The second through the fifth ribs probably articulated distally with the ossified sternal ribs preserved in the referred specimen. The tuberculum of the second rib is long and set at nearly a right angle to the rib shaft and capitulum. The mid- and caudal thoracic rib shafts decrease in width and length but retain an oval cross section.

Portions of the shafts of the caudal thoracic ribs were previously interpreted as gastralia (Fig. 8.4; Sereno and Rao, 1992). These apparently short and tapered elements are best identified as caudal thoracic rib shafts that are passing into, and out of, the part slab. Their shafts are comparable to those of nearby ribs, rather than being much more slender, as are the gastralia in *Archaeopteryx* and *Confuciusornis* (Chiappe et al., 1999). The absence of gastralia is now demonstrated in the articulated skeletons of other very well-preserved enantiornithines, such as *Concornis* (Sanz et al., 1995) and *Eoalulavis* (Sanz et al., 1996), and we believe that *Sinornis* is no exception.

Chevrons. All the free caudal vertebrae are associated with chevrons (Fig. 8.2). The first chevron articulates between the eighth sacral and first caudal, as shown by the pair of large articular facets along the cranial margin of the first caudal vertebra. The last chevron is as long as, or longer than, the others and articulates between the fifth and sixth caudal vertebrae.

Pectoral Girdle

Scapula. The scapula closely resembles that of *Concornis* and is preserved in both specimens. Cranially, a robust, subrectangular acromial process projects away from the axis of the scapular blade at an angle of approximately 45°. The scapular glenoid has a gently concave, kidney-shaped surface. When the scapular blade is held in a horizontal plane, the glenoid faces primarily laterally and slightly dorsally, as reported (Zhou, 1995a:12). It also is canted to face slightly cranially. The costal (dorsal) and lateral (ventral) margins of the blade are gently arched and straight, respectively. The blade is broadest about two-thirds of the way down its length and tapers to a rounded distal end (IVPP V9769A).

Coracoid. Very little of the coracoid is exposed in the holotypic specimen. The coracoids of the referred specimen, however, are well exposed and resemble those in other enantiornithines (Chiappe and Walker, Chapter 11 in this volume). A rounded and very prominent acrocoracoid process projects dorsally from the proximal end of the coracoid. The shaft broadens distally into a curved sheet of bone with convex cranial, and concave caudal, surfaces. The lateral margin is convex. The straight distal articular edge for the sternum is offset slightly from a perpendicular to the axis of the coracoid.

Furcula. The robust Y-shaped furcula is exposed in both holotypic and referred specimens. The clavicular rami join ventrally, with an intrafurcular angle of approximately 50°. The long hypocleideum is blade-shaped with sharp cranial and caudal margins. In both specimens, the edges of the hypocleideum join a crest along the edge of each dorsal ramus. The shaft is flattened near the distal end of the dorsal ramus and curves laterally toward the acromion, as in *Concornis* (UAM LH-2814). Given the prominence of both the scapular acromion and coracoidal acrocoracoid process, there can be little doubt that the curved articular end of the dorsal process of the furcula completed a triosseal canal that would have accommodated the tendon of the supracoracoideus muscle, as in living birds.

Sternum. The broad plate-shaped sternum is partially preserved in ventral view in the holotypic specimen and nearly fully exposed in dorsal and ventral views in the referred specimen. The cranial margin is thickened with broad, trough-shaped articular surfaces for the coracoids (IVPP V9769B). A short median slit accommodates the dorsal edge of the hypocleideum of the furcula as in *Eoalulavis* (Sanz et al., 1996). The slender caudolateral processes flare at their distal ends, and the caudal margin of the sternum is W-shaped (Zhou, 1995a: Fig. 5a), as in *Concornis* (Sanz et al., 1995).

Forelimb

Humerus. The holotypic specimen preserves the proximal and distal ends of the right humerus. Both humeri are preserved in the referred specimen. At the proximal end, both specimens show the hypertrophied bicipital tubercle that characterizes enantiornithines (Walker, 1981; Chiappe, 1996). In the holotypic specimen, this tubercle has a curved columnar form with a concave distal end, as in *Eoalulavis* (UAM LH 13500; Sanz et al., Chapter 9 in this volume). The distal condyles of the humerus are similar to those in other enantiornithines. In both specimens, the radial condyle is transversely narrower and more prominent than the ulnar condyle, but the radial condyle is not shifted significantly proximally as in Neornithes. The ulnar condyle is broad and has a distinctly flattened articular surface. The saddle-shaped form of the humeral head and other features are characteristic of enantiornithines and are well described elsewhere (Chiappe, 1996).

Radius and Ulna. The radius and ulna are well exposed in the referred specimen; in the holotypic specimen, the left forearm is folded against the humerus, and the right forearm is preserved only proximally. The radius and ulna are very similar to those in *Concornis, Eoalulavis,* and other enantiornithines (Chiappe, 1996; Chiappe and Walker, Chapter 11 in this volume). The slightly expanded proximal end of the radius has an oval proximal articular surface, a subtriangular facet for the ulna, and a low biceps tuberosity (IVPP V9769A). The radial shaft is marked by a shallow groove (Zhou, 1995a:13) as in other enantiornithines and *Ichthyornis.* The distal end is curved and strongly flattened, with a narrow distal articular surface.

The ulnar shaft has a minimum width approximately twice that of the radius. The proximal one-third of the shaft curves toward the elbow joint. A biceps tubercle is located just before this articulation. The distal end has an arcuate external condyle and a trough-shaped intercondylar sulcus, as noted by Zhou (1995a:18). There are no papillae for flight feathers on the shaft of the ulna in either specimen.

Proximal Carpals. The radiale and ulnare have yet to be described in detail among enantiornithines. Both ossifications are preserved in the holotypic specimen, although only the form of the radiale is well shown. Initially identified as the ulnare (Sereno and Rao, 1992: Fig. 3E), the left radiale of the holotypic specimen is preserved disarticulated a short distance from the wrist joint. Its concave, heart-shaped distal articular surface is exposed. In the referred specimen, the right radiale is also disarticulated a short distance from the wrist joint and is exposed in proximal and distal views. The left radiale, however, is in place at the distal end of the ulna, with its concave, heart-shaped distal articular surface exposed. This surface articulates against the convex trochlea of the semilunate carpal.

The left ulnare is present in the holotypic specimen but not well exposed. It is preserved in place on the external side of the left wrist joint, articulating in the angle between the forearm and manus. It appears to have been similar to the large V-shaped ulnare in the enantiornithines *Eoalulavis* (UAM LH 13500; Sanz et al., 1996) and *Neuquenornis* (Chiappe and Calvo, 1994: Fig. 1), in the euornithine *Ichthyornis* (Marsh, 1880: Pl. 30), and in Neornithes. The internal surface of this V-shaped bone forms a deep articular notch for the metacarpus, an unusual configuration that is absent in *Archaeopteryx* and only poorly formed in *Confuciusornis.* In the latter, the ulnare has a broader trough shape and is only about one-half the size of the radiale. An enlarged V-shaped

ulnare, therefore, appears to have evolved in basal ornithothoracines (Sereno, 1999a: Fig. 4).

Carpometacarpus. The carpometacarpus is preserved in both specimens and is at least partially co-ossified. Prior to acid preparation of the holotypic specimen, the fragmented base of the right carpometacarpus gave the appearance that metacarpal II and the semilunate carpal had yet to co-ossify (Fig. 8.3; Sereno and Rao, 1992:845). This portion of the carpometacarpus is better preserved on both sides of the referred specimen, in which metacarpal II and the semilunate carpal are clearly co-ossified. The same is not uniformly true of metacarpal I, which in the left manus of the holotypic specimen is disarticulated, lying near the base of metacarpal III (Fig. 8.3). The length of the disarticulated left metacarpal I, however, suggests that it may include part of the semilunate carpal, which may have broken away from the remainder of the carpometacarpus. In the right carpometacarpus of the holotypic specimen, the distal condyles of right metacarpal I are in their proper position alongside metacarpal II, but the base of the bone has broken away. In the referred specimen, metacarpal I is preserved in place in both manus and appears to be co-ossified with the medial edge of the semilunate carpal. The trochlea of the semilunate carpal is situated largely proximal to metacarpal II.

Metacarpal I is very short, although longer than that shown in an enantiornithine from Argentina (Walker, 1981: Fig. 2F). The medial margin of the proximal half of the shaft is convex and may constitute a rudimentary extensor process (IVPP V9769A), similar to that seen in *Confuciusornis, Archaeopteryx,* and many nonavian maniraptorans. The distal condyles are best exposed in the holotypic specimen and closely resemble those in *Archaeopteryx;* the deeper medial distal condyle projects farther distally and is raised above the level of the medial condyle. These features, and the well-developed dorsal extensor depression between the condyles, indicate that the phalanges of the first digit were deflected medially and were capable of substantial rotation against the metacarpal.

Metacarpal II is the most robust. The shaft appears to be subquadrate in cross section but is dorsoventrally flattened in sections by postmortem crushing. There is no dorsal extensor depression distally. Distal condyles are not apparent in dorsal view, because they are beveled proximoventrally. The distal condylar surface is developed as a broad saddle, with the condyles canted medially.

An interosseous space separates metacarpal III from metacarpal II, and, although fused proximally, these bones remain separate distally. As in most neornithines, the shaft of metacarpal III is transversely flattened, particularly in its proximal one-half. The shaft, therefore, is readily deflected by postmortem crushing, a situation that has given rise to spurious interpretations, such as the absence of an interosseous space in *Sinornis* (Zhou, 1995a: Fig. 8) or the notion that the shaft is as robust as that of metacarpal II in *Neuquenornis* (Chiappe and Calvo, 1994:236). As in other enantiornithines (Chiappe and Walker, Chapter 11 in this volume) and some neornithines, metacarpal III is longer than metacarpal II, and the medially curving shaft terminates in subequal distal condyles, as seen in both specimens.

Phalanges. The phalangeal formula is 2-3-1, with digits I and II terminating in recurved unguals (Fig. 8.3; Zhou, 1995a). Although the manual phalanges are completely preserved in *Sinornis,* evidence from other enantiornithines is consistent with this pattern (e.g., *Concornis, Eoalulavis*).

The first phalanx of digit I is long, slender, and gently arched dorsoventrally. The distal end has well-developed condyles, extensor and flexor pits, and medial and lateral collateral ligament pits. The ungual is slightly shorter and more recurved than that on digit II (Fig. 8.3). The tip of the ungual of digit I falls short of the length of metacarpal II, suggesting that digit I may be relatively shorter in *Sinornis* than in some other enantiornithines (e.g., *Eoalulavis*).

The first phalanx of digit II has a concave proximal articular surface, weakly divided into two unequal articular facets (IVPP V9769). A proximally projecting heel is present on the ventral aspect of the base, distal to which is located a large foramen and associated canal (Fig. 8.3). This unusual foramen, which has never been reported before among avians, is present in both the holotypic and referred specimens and in the enantiornithine *Eoalulavis* (UAM LH 13500). It may have accommodated a flexor tendon on the ventral aspect of the digit in some as yet poorly understood configuration; the foramen and canal seem too large to have transmitted neurovascular structures and are difficult to envision as a pneumatic invasion of the phalanx (Sereno, 2000). A flange is present on the lateral side of the distal two-thirds of the shaft, and, as a result, the phalanx appears to broaden in width distally until just before the condyles. The distal condyles are weakly separated, and there are no extensor and flexor depressions or collateral ligament pits.

The second phalanx of digit II tapers distally, although, as in the preceding phalanx, a lateral flange is present. The distal trochlea is well developed and symmetrical, with extensor and flexor depressions and collateral ligament pits (Fig. 8.3). The ungual is larger and less recurved than that of the first digit, although both unguals are relatively shorter and less recurved than those in *Archaeopteryx* and *Confuciusornis.*

The sole phalanx of digit III is anchored laterally against the shaft of the first phalanx of digit II (Fig. 8.3). In the holotypic specimen, only the proximal third of the shaft articulates against the adjacent phalanx. The remainder of the shaft curves away (Fig. 8.3). In the referred specimen, left

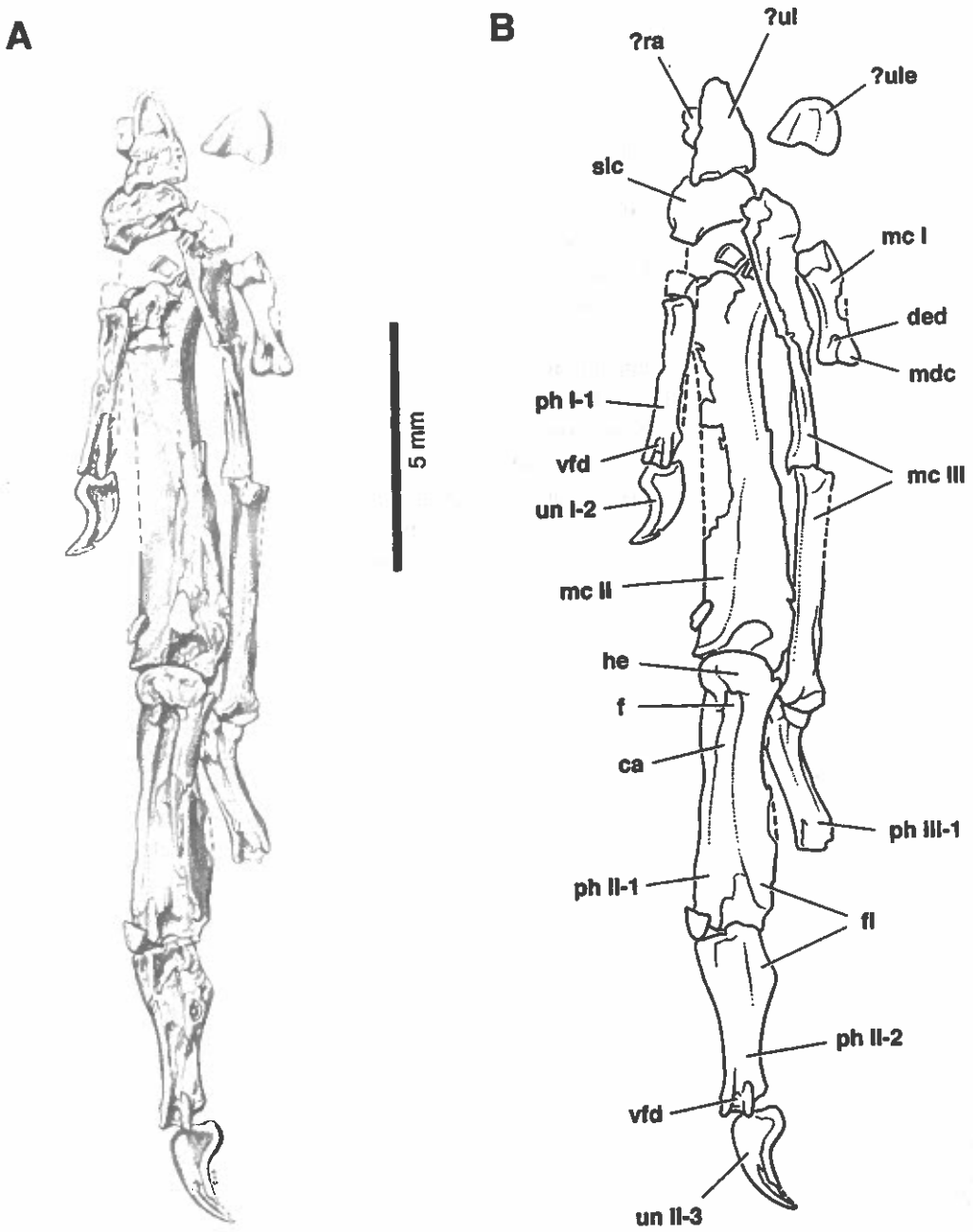

Figure 8.3. Right carpus and manus of *S. santensis* (BPV 538a, epoxy cast), mostly in ventral view (A, B). Metacarpal I is in dorsal view, digit I ungual is in medial view, and digit II ungual is in lateral view. Broken lines indicate bone margins visible as impressions. Abbreviations: I–III, metacarpals or digits I–III; 1–3, phalangeal number; ca, canal; ded, dorsal extensor depression; f, foramen; fl, flange; he, heel; mc, metacarpal; mdc, medial distal condyle; ph, phalanx; ra, radius; slc, semilunate carpal; ul, ulna; ule, ulnare; un, ungual; vfd, ventral flexor depression.

and right sides show a different pattern. There is a narrow medial flange that contacts the adjacent phalanx along most of its straighter shaft. Only the narrow distal end is free and, despite the absence of an additional ossified phalanx, appears to be developed as a rudimentary condyle.

Pelvic Girdle

In the holotypic specimen, the right half of the pelvic girdle has been displaced ventrally relative to the left side, and the sacrum has been rotated to expose its ventral side (Fig. 8.4). In the referred specimen, the pelvic girdle is completely disarticulated. It is clear that the pelvic girdle and sacrum were not fully co-ossified in either specimen. The natural configuration of the pelvic girdle is best preserved on the left side of the holotypic specimen, where two of the three main articulations (iliopubic and ilioischiadic) appear to be co-ossified. The ischiadic and pubic shafts parallel each other, and the pubic shaft is rotated significantly caudal to a vertical orientation. The acetabulum is broadly open medially.

Ilium. The ilium has a deep preacetabular process and a narrower, arched postacetabular process (Fig. 8.4) as in other enantiornithines (Walker, 1981; Sanz et al., 1996; Sereno, 2000; Chiappe and Walker, Chapter 11 in this volume). The pubic peduncle is longer than the ischiadic peduncle, as in *Archaeopteryx* and many other paravians. The pubic peduncle is narrower craniocaudally than in *Archaeopteryx* (Wellnhofer, 1974), *Rahonavis* (Forster et al., 1998), and dromaeosaurids but is quite similar to that in *Confuciusornis*. Well-developed dorsal and ventral antitrochanters are present on the dorsal margin and ischiadic peduncle of the ilium, respectively. The ventral antitrochanter is prominent (Fig. 8.4); it is partially broken away in the exposed left ilium of the referred specimen, which is why its presence was formerly questioned (Zhou, 1995a:13). As in other enantiornithines, the dorsal rim of the postacetabular process caudal to the dorsal antitrochanter projects laterally (Fig. 8.4; Walker, 1981: Fig. 2C).

Ischium. The iliac peduncle of the ischium is articulated with the ilium in the holotypic specimen (Fig. 8.4). The ventral antitrochanter is shared between these bones, the ventral one-quarter of which forms a raised platform on the acetabular margin of the ischium. The remainder of the acetabular margin of ischium is rounded and tapers in width toward the end of the pubic peduncle, which is developed as a broad, thin sheet of bone.

The proximodorsal process of the ischium is developed as a tongue-shaped flange, the tip of which articulates on the medial aspect of the postacetabular process of the ilium. The elongate ischiadic blade is scimitar-shaped, gradually tapering toward its gently curved tip. At its narrowest width, the blade is approximately one-tenth of total ischiadic length. The distal portion of the blade is exposed on the right side of the holotypic specimen (Fig. 8.4). A reflected lamina is present on the lateral side of the blade, an unusual feature that can also be observed on the left ischium of the referred specimen (IVPP V9769B). At its proximal end, the reflected lamina is about one-half the width of the blade. Distally, the lamina decreases in width to form the laterally protruding dorsal margin of the distal one-half of the blade. The shorter length of the ischiadic blade in a previous reconstruction (Zhou, 1995a: Fig. 10B) was based on the incomplete distal ends of the ischia of the referred specimen.

Pubis. The pubis is longer than the ischium. Its cranial margin, from the iliac peduncle to the foot, is gently curved caudally. The acetabular margin of the pubis is broad and joins the prominent supracetabular crest of the ilium (Fig. 8.4). The plate-shaped ischiadic peduncle is very short; its height exceeds its length. The proximal one-half of the pubic shaft appears to have a subtriangular cross section; the medial side is flattened, and a rounded edge is present laterally. The distal two-thirds of the shaft is blade-shaped, with a rounded lateral edge and sharp medial edge. Proximal to the foot, the blade expands in width, as is best exposed in the right pubis of the holotypic specimen (Fig. 8.4). This well-preserved distal end suggests that the pubic symphysis, which had yet to co-ossify in either specimen, was limited to the distal one-quarter of the pubic blade. The subtriangular pubic foot curves caudally.

Hindlimb

Femur. The femoral head is approximately 60% the maximum craniocaudal width of the femur; it is not particularly small in this regard. It is separated from the greater trochanter by a shallow articular saddle. A prominent caudal trochanter, preserved in both femora of the referred specimen, is present on the caudolateral side of the proximal end, distal to the greater trochanter. A trochanter of similar position and size is present in *Archaeopteryx* and other basal paravians. The shaft is very gently caudally curved. There is no trace of a fourth trochanter. The distal condyles are subequal in size and separated caudally by the popliteal fossa. The lateral distal condyle has a distinct caudal extension, the crista tibiofibularis (IVPP V9769A).

Tibiotarsus. The proximal articular surface is oval, only slightly longer craniocaudally than broad. The proximal end of the tibiotarsus appears to have a very low, laterally projecting cnemial crest, separated proximally from the remainder of the proximal articular surface by a shallow groove (contra Zhou, 1995a:14). This area is only preserved in the tibiae of the referred specimen and has suffered some crushing (IVPP V9769A, B). The fibular crest projects from the lateral aspect of the shaft as a thin flange, reaching its

Figure 8.4. Sacral and cranial caudal vertebrae, caudal dorsal ribs, and pelvic girdle of *S. santensis* (BPV 538a, epoxy cast), as shown in full-tone (A) and outline (B) drawings. Vertebrae are in ventral view, and pelvic elements are in left lateral view. Broken lines indicate bone margins visible as impressions. Abbreviations: acet, acetabulum; ach, articular surface for chevron; c, centrum; ca1, first caudal vertebra; dant, dorsal antitrochanter; dpr, proximodorsal process; fe, femur; fl, flange; il, ilium; is, ischium; pfo, pubic foot; poap, postacetabular process; pped, pubic peduncle; prap, preacetabular process; pu, pubis; r, rib (also right); s1–8, sacral vertebrae 1–8; sym, symphyseal surface; tp, transverse process; vant, ventral antitrochanter.

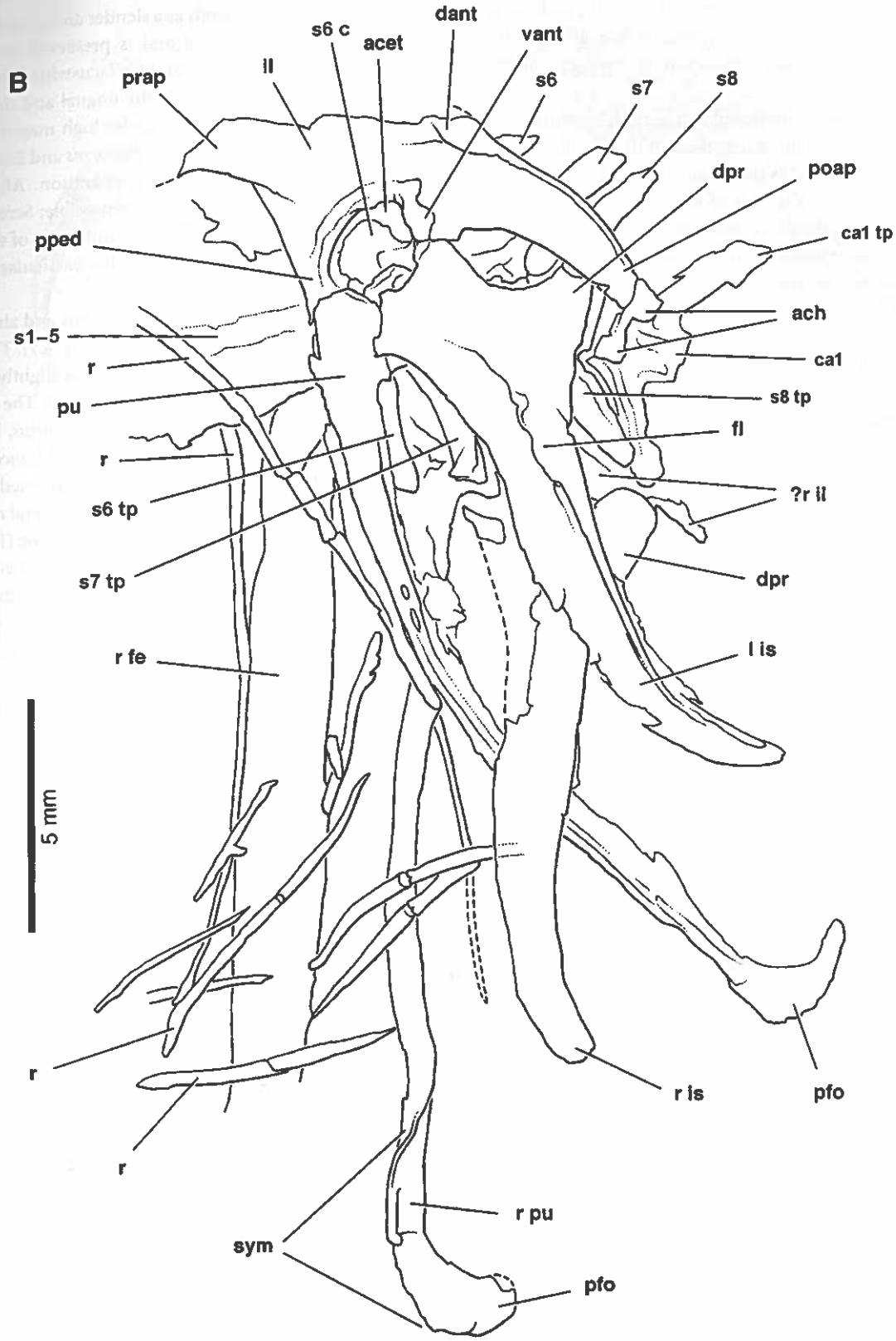
B
prap
il
s6 c
acet
dant
vant
s6
s7
s8
dpr
poap
ca1 tp
pped
ach
s1–5
ca1
r
pu
s8 tp
fl
r
?r il
s6 tp
s7 tp
dpr
r fe
l is
5 mm
r
r is
pfo
r
r pu
sym
pfo

broadest width near its distal end. The distal condyles are large; in side view, the lateral condyle is nearly circular, whereas the medial condyle projects more strongly caudally.

Fibula. The fibula, disarticulated in both specimens, extends along only the upper one-third of the tibiotarsus. The flattened proximal end is triangular, the caudal corner projecting farther from the axis of the shaft (IVPP V9769B). The iliofibularis tubercle is developed as a distinct swelling on the craniolateral margin of the shaft (BPV 538a). Distal to this tubercle, the shaft tapers into a narrow rod that extends a short distance beyond the fibular crest on the tibia.

Tarsometatarsus. The tarsometatarsi of the holotypic specimen are well preserved and exposed, showing the distal, fully retroverted (anisodactyl) position of digit I. Zhou (1995a:14) described the absence of a hypotarsus and commented on the length and form of metatarsal II in the referred specimen (IVPP V9769B), which shows the expanded, medially deflected distal condyles that characterize the holotypic specimen and most other enantiornithines (Chiappe, 1993). Co-ossified distal tarsals appear to form a slightly expanded cap fused to the proximal ends of metatarsals II–IV, although no sutures remain. A very short section of the suture between the proximal ends of metatarsals II and III is also co-ossified. This co-ossification has maintained the integrity of the tarsometatarsi in both specimens.

Metatarsal I has a splint-shaped shaft and is located at the distal end of metatarsal II (Figs. 8.5–8.7). On the right side of the holotypic specimen, digit I has shifted caudally, so that metatarsal I is in contact with metatarsal IV (Fig. 8.6). In side view, metatarsal I is J-shaped as a result of its bulbous distal condyle, which is single cranially but divided by a groove caudally. A broad, asymmetrical dorsal extensor depression is present just behind the condyle, and the collateral ligament pit is deeper on the medial side.

Metatarsals II–IV are very similar to those in other basal enantiornithines, such as *Iberomesornis* (Sanz and Bonaparte, 1992; Sereno, 2000; Sanz et al., Chapter 9 in this volume) and *Concornis* (Sanz et al., 1995). A suite of derived enantiornithine features include the very broad distal condyles of metatarsal II (Fig. 8.6), the caudally prominent medial distal condyle of metatarsal III (Fig. 8.7), extremely narrow shaft of metatarsal IV (Fig. 8.5), and C-shaped distal condyles of metatarsal IV (Chiappe, 1993, 1996). The derived form of metatarsal I and the reduced size of metatarsal IV are also visible in the referred specimen (IVPP V9769B). Metatarsal V is absent.

Phalanges. The pedal phalanges are articulated and well exposed in the holotypic specimen. The phalangeal formula is 2-3-4-5-*x* (Figs. 8.5, 8.6). Horny claw sheaths are partially preserved, especially the hard outer rim (Figs. 8.5–8.7). This keratinized outer rim extends as a slender arcuate extension from the tip of each ungual and is preserved in several enantiornithine specimens encased in lacustrine sediments. The juncture between the tip of the ungual and the outer rim of the claw sheath is visible under high magnification in the holotypic specimens of *Iberomesornis* and *Concornis*, which have not undergone acid preparation. After acid preparation, such a distinction is not possible; Sereno and Rao (1992) misinterpreted the slender outer rim of the claw sheaths in the holotypic specimen as the particularly slender tips of the pedal unguals.

The proximal phalanx of digit I is robust and almost as long as the proximal phalanx of digit III (Fig. 8.7). The base is very broad, and the lateral distal condyle is slightly longer than the medial distal condyle, as in *Concornis*. The ungual is as long and recurved as that in digit II. *Sinornis*, like the other basal enantiornithines *Iberomesornis* and *Concornis*, is characterized by a robust, long, and fully retroverted digit I.

The phalanges of digit II are distinctive in several regards. The proximal phalanx has a particularly broad base (Fig. 8.6) to accommodate the transversely expanded distal condyles of metatarsal II. The penultimate phalanx is longer than that proximal to it, as in digits III and IV. Its distal condyles are more expanded and the intercondylar depression is deeper than comparable phalanges of digits III or IV (either the second or penultimate phalanges). Likewise, the ungual is more recurved and the flexor tubercle significantly more robust than the unguals in digits III or IV (Figs. 8.5, 8.6). These features are also present in *Archaeopteryx* (Wellnhofer, 1974: Fig. 13) and *Confuciusornis* and may well be homologous with the similar, but hypertrophied, condition of digit II in *Rahonavis* (Forster et al., 1998) and basal paravians, such as dromaeosaurids and troodontids (Sereno, 1999a).

The proximal phalanx of digit III is the most robust nonungual phalanx in the pes. The second phalanx is shorter, and the penultimate phalanx is as long as, but more slender than, the first phalanx. The ungual is the longest in the pes.

The first two phalanges of digit IV are subequal in length (Figs. 8.5, 8.7), whereas the second is significantly shorter in *Archaeopteryx* and *Confuciusornis* (Chiappe et al., 1999). The third phalanx is somewhat shorter, and the penultimate phalanx is much longer. These proportional differences are readily understood as adaptations that enhance perching function (Hopson and Chiappe, 1998; Hopson, 2001). The ungual is shorter than that of digits I–III and is the least recurved in the pes.

Phylogenetic Relationships

Basal Avian Relationships

Recent years have witnessed a profound transformation in the quality of the early avian fossil record, as this volume at-

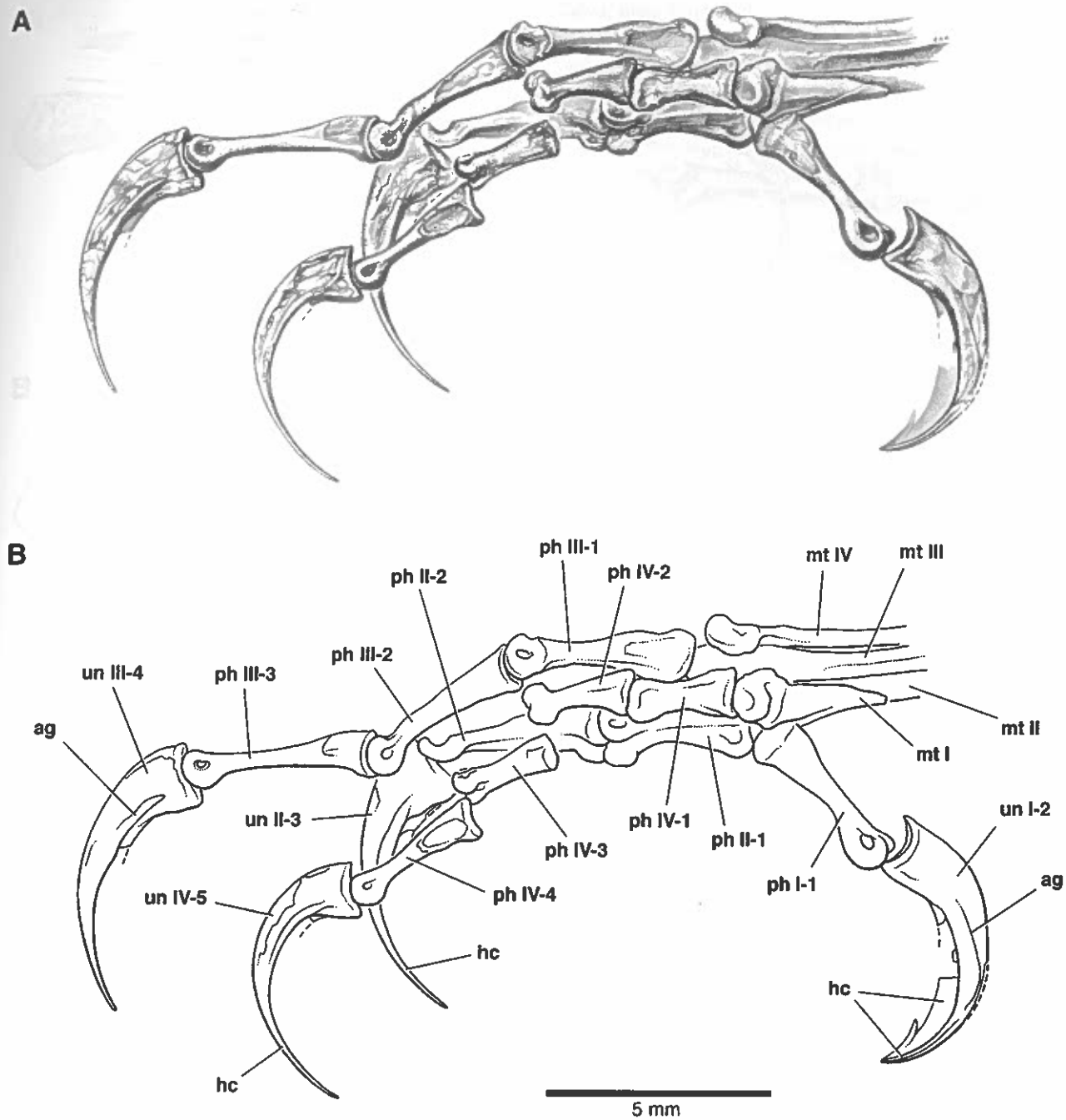

Figure 8.5. Left distal metatarsals (most in dorsal view) and pedal phalanges (most in medial view) of *S. santensis* (BPV 538a, epoxy cast) (A, B). Broken lines indicate the margins of bone or horny claw that are visible as impressions. Abbreviations: I–IV, metatarsals or digits I–IV; 1–5, phalangeal number; ag, attachment groove; hc, horny claw; mt, metatarsal; ph, phalanx; un, ungual.

tests. Despite the presence of several taxa of uncertain association or controversial affinity, such as *Protoavis* (Chatterjee, 1995) and the alvarezsaurids (Chiappe et al., 1996; Novas, 1997; Sereno, 1997, 1999a, 2001; Chiappe et al., 1998), a phylogenetic framework has emerged (Chiappe, 1995, 1996; Sereno 1997, 1999a; Chiappe et al., 1998). This framework (Fig. 8.9C) constitutes a consensus of recent cladistic analyses with explicit outgroups that attempt to incorporate the increasing quantity of skeletal data now available. In a recent analysis (Sereno, 1999a), for example, approximately 100 synapomorphies have been identified in support of three nodes at the base of Aves (Fig. 8.9C).

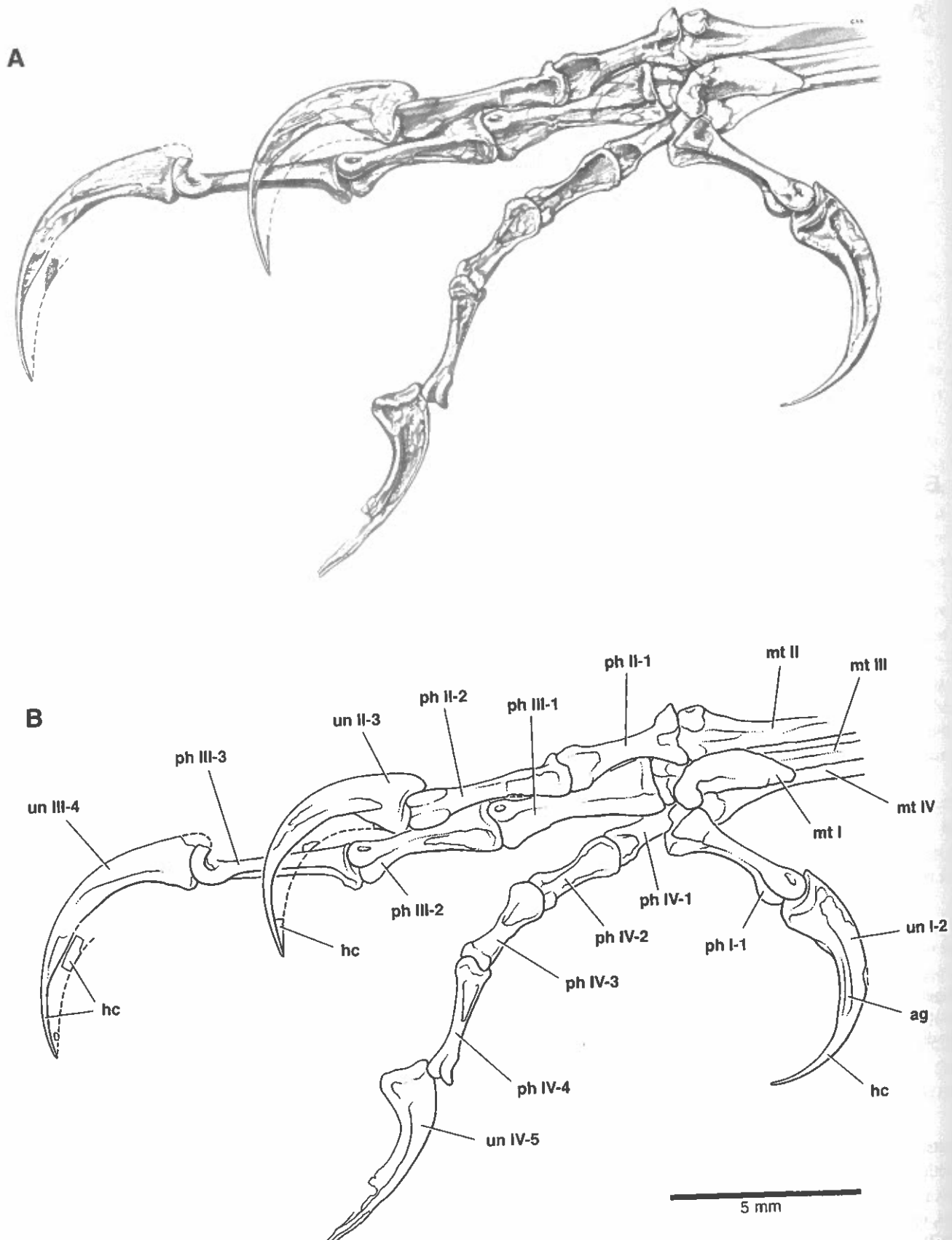

Figure 8.6. Right distal metatarsals and pedal phalanges of *S. santensis* (BPV 538a, epoxy cast), most in ventral view (A, B). Broken lines indicate the margins of bone or horny claw that are visible as impressions. See Figure 8.5 for abbreviations.

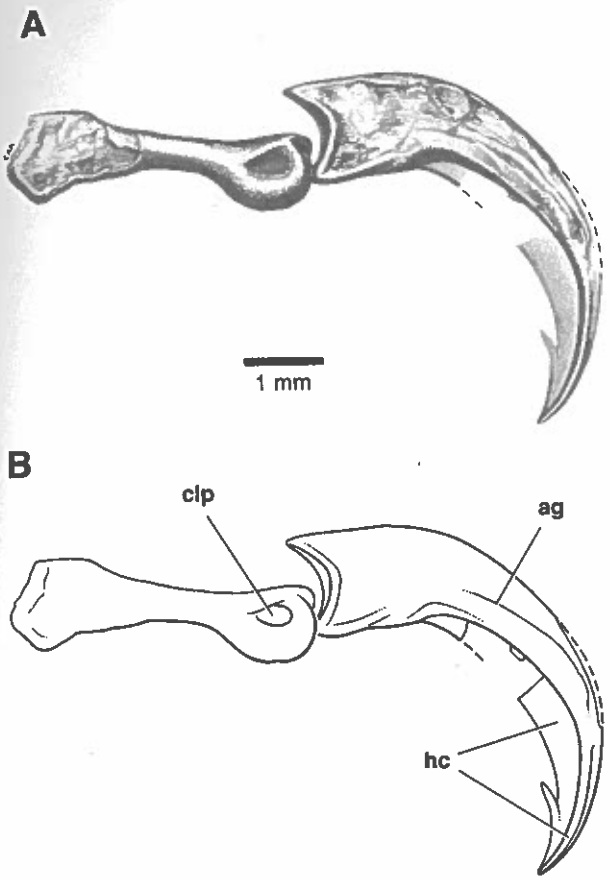

Figure 8.7. Left pedal digit I phalanges of *S. santensis* (BPV 538a, epoxy cast) in lateral view (A, B), showing the side of digit I that is farthest from digit II. Broken lines indicate the margins of bone or horny claw that are visible as impressions. Abbreviations: clp, collateral ligament pit; ag, attachment groove; hc, horny claw.

Enantiornithine Status of *Sinornis*

Sereno and Rao (1992) initially described the holotypic specimen of *S. santensis* as the most basal avian after *Archaeopteryx* (Fig. 8.10A). At that time, articulated remains of other basal avians were rare and included only *Ambiortus* (Kurochkin, 1985), a partial postcranial skeleton from Mongolia, and *Iberomesornis* (Sanz et al., 1988; Sanz and Bonaparte, 1992), a more complete postcranial skeleton from Spain. It is now clear that the two features used by Sereno and Rao (1992) to establish the basal position of *Sinornis* relative to *Ambiortus* and *Iberomesornis*—the presence of gastralia and a plate-shaped coracoid—were based on misidentifications (of rib tips and a portion of the left humerus, respectively).

Sereno and Rao (1992) did not compare *Sinornis* with the available disarticulated material of enantiornithines (Walker, 1981; Molnar, 1986). As more complete enantiornithine remains came to light (Chiappe, 1991, 1993; Sanz and Buscalioni, 1992; Zhou et al., 1992, 1995a; Chiappe and Calvo, 1994; Sanz et al., 1995), the status of *Sinornis* as an enantiornithine was proposed (Chiappe, 1995; Zhou, 1995a). *Ambiortus* and *Iberomesornis*, in turn, also appear to belong within Enantiornithes. Initially, these genera were allied with Enantiornithes based on overall similarity rather than synapomorphy (Martin, 1995; Kurochkin, 1996). More recently, several enantiornithine synapomorphies were highlighted in a revision of the skeletal anatomy of *Iberomesornis* (Sereno, 2000).

Enantiornithine synapomorphies were first outlined by Walker (1981) and Chiappe (1991, 1993) based largely on disarticulated material. Chiappe and Calvo (1994) and Chiappe (1996) listed 21 and 22 synapomorphies, respectively. Kurochkin (1996:32–33) listed 34 characters in his diagnosis of Enantiornithes, but these constitute a mixture of enantiornithine synapomorphies and symplesiomorphies that characterize many other avians (e.g., "digit I reversed").

Sereno (2000) accepted 12 of the 22 synapomorphies listed by Chiappe (1996:213) and added another 15 for a total of 27 enantiornithine synapomorphies. Most of these 27 synapomorphies are present in *S. santensis*, but the following 19 are the easiest to observe in the postcranial skeleton (Fig. 8.8; BPV 538a; IVPP V9769A, B). In the axial column, (1) the parapophyses of cranial dorsal vertebrae are positioned in the center of the centrum. In the pectoral girdle, (2) the dorsolateral rami of the furcula are L- or V-shaped in cross section; (3) the hypocleideum is 40% or more of the length of the dorsolateral ramus of the furcula; (4) the scapular acromial process is deflected medially at about 45° from the long axis of the scapula; and (5) the ventral ramus of the coracoid has a convex lateral margin and is transversely arched. In the forelimb, (6) the proximal apex of the humeral head is gently saddle-shaped; (7) the internal tuberosity (located on the proximal end of the humerus ventral to the head) is associated with a pneumatic opening; (8) a humeral dorsal trochanter is present; (9) the humeral ventral trochanter is developed as a pendant process with a subtriangular cross section and terminal fossa; (10) humeral distal condyles with transverse axis angled ventromedially at approximately 25° from the perpendicular to the shaft axis; (11) humeral distal end with maximum width across the epicondyles three times maximum craniocaudal depth; and (12) foramen present on the ventral aspect of the base of manual phalanx II-1. In the pelvic girdle, (13) the iliac postacetabular process has a maximum depth one-third the maximum depth of the preacetabular process. In the hindlimb, (14) the distal condyles of metatarsal I are reflected caudally; (15) the distal condyles of metatarsal I are joined along their dorsal margin; (16) the distal condyles of metatarsal II and the proximal articular surface of opposing phalanx II-1 are broader in width than those of metatarsal III and phalanx III-1; (17) the medial distal condyle of metatarsal III extends significantly caudal to the lateral

Figure 8.8. Silhouette reconstruction of *S. santensis* showing the preserved bones, based on BPV 538 and IVPP V9769.

condyle; (18) the distal shaft of metatarsal IV is much narrower than that of metatarsals II and III; and (19) the distal condyles of metatarsal IV are C-shaped in distal view. These synapomorphies were adapted from Chiappe, 1991 (synapomorphy 5); Chiappe, 1993 (synapomorphies 14, 16–19); Chiappe and Calvo, 1994 (synapomorphies 6, 11); Chiappe, 1996 (synapomorphies 1, 2); and Sereno, 2000 (synapomorphies 3, 4, 7–10, 12, 13, 15).

Relationships within Enantiornithes

What are the relationships of *S. santensis* within Enantiornithes? Enantiornithine relationships have been considered by Chiappe (1993), Sanz et al. (1995), and Kurochkin (1996). These studies highlight just how little is known about the internal structure of this major avian radiation.

Chiappe (1993) described 10 characters in six enantiornithine genera, using *Mononykus* and *Patagopteryx* as outgroups (Fig. 8.10B). Three of these characters (1, 4, 10) are enantiornithine synapomorphies and, as scored by Chiappe (1993: Fig. 13), are uninformative regarding relationships among enantiornithines. Three of the remaining characters (2, 5, 6; metatarsal I distal condyles strongly reflected or "J-shaped"; caudally extended medial distal condyle on metatarsal III; and metatarsal IV distal condyles C-shaped)

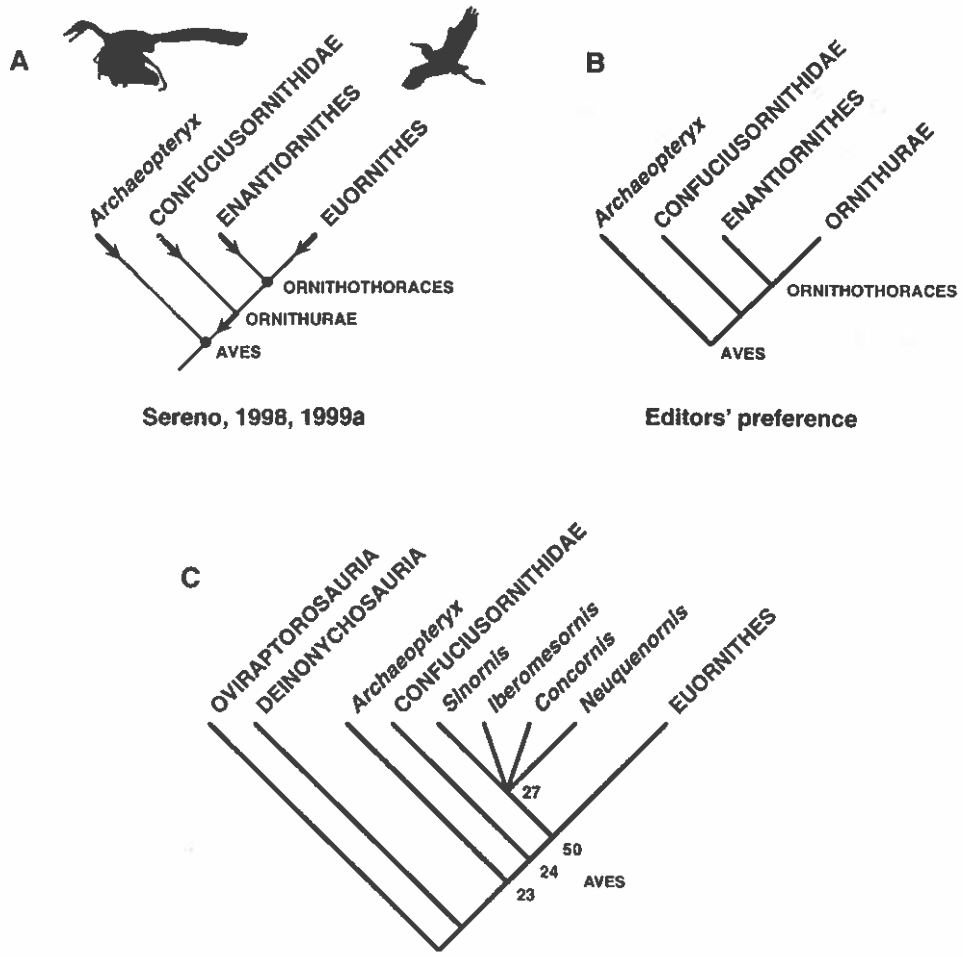

Figure 8.9. Basal avian taxonomy and phylogeny. (A) Higher-level avian taxonomy (from Sereno, 1998, 1999a). Dots and arrows indicate taxa with node-based and stem-based definitions, respectively. Euornithes Dementjev 1940 was inadvertently listed as a new taxon (Sereno, 1998). (B) Editors' preferred higher taxonomy for the same basal phylogeny as in (A), differing in use of the taxon Ornithurae. (C) Higher-level avian phylogeny, with number of synapomorphies shown at each node (under delayed character-state optimization). Alvarezsaurids are regarded as ornithomimosaurs (and so are not included on the cladogram; Sereno, 1999a, 2000), and *Iberomesornis* is regarded as an enantiornithine (Sereno, 2000).

we also regard as enantiornithine synapomorphies; these features, for example, are present in *Sinornis*. One of the remaining characters (4; tubercle for the tibialis cranialis muscle on metatarsal II) is probably plesiomorphic within Enantiornithes, given its presence in the outgroups *Confuciusornis* and dromaeosaurids (Norell and Makovicky, 1997:10–11, Fig. 6). Although Chiappe correctly reported three minimum-length (12-step) trees with a consistency index of 0.83, the robustness of this result was not considered. If the data as presented are accepted, all structure among enantiornithines breaks down with one additional step (13 steps, 17 trees; Fig. 8.10B).

Sanz et al. (1995) added *C. lacustris* to the matrix in Chiappe (1993), using the same 10 characters and pair of outgroups (Fig. 8.10C). Their results were the same: three minimum-length trees with the same consistency index. After examining the holotypic skeleton of *Concornis*, we would score four characters (2, 4, 6, 7) with the derived state (as opposed to primitive or missing states). Nonetheless, if the data as originally presented are accepted, all structure within Enantiornithes breaks down with one additional step (13 steps; 32 trees; Fig. 8.10C). This is not the result of a single incomplete taxon. If *Lectavis*, the least complete taxon in the matrix (50% complete), is removed, all struc-

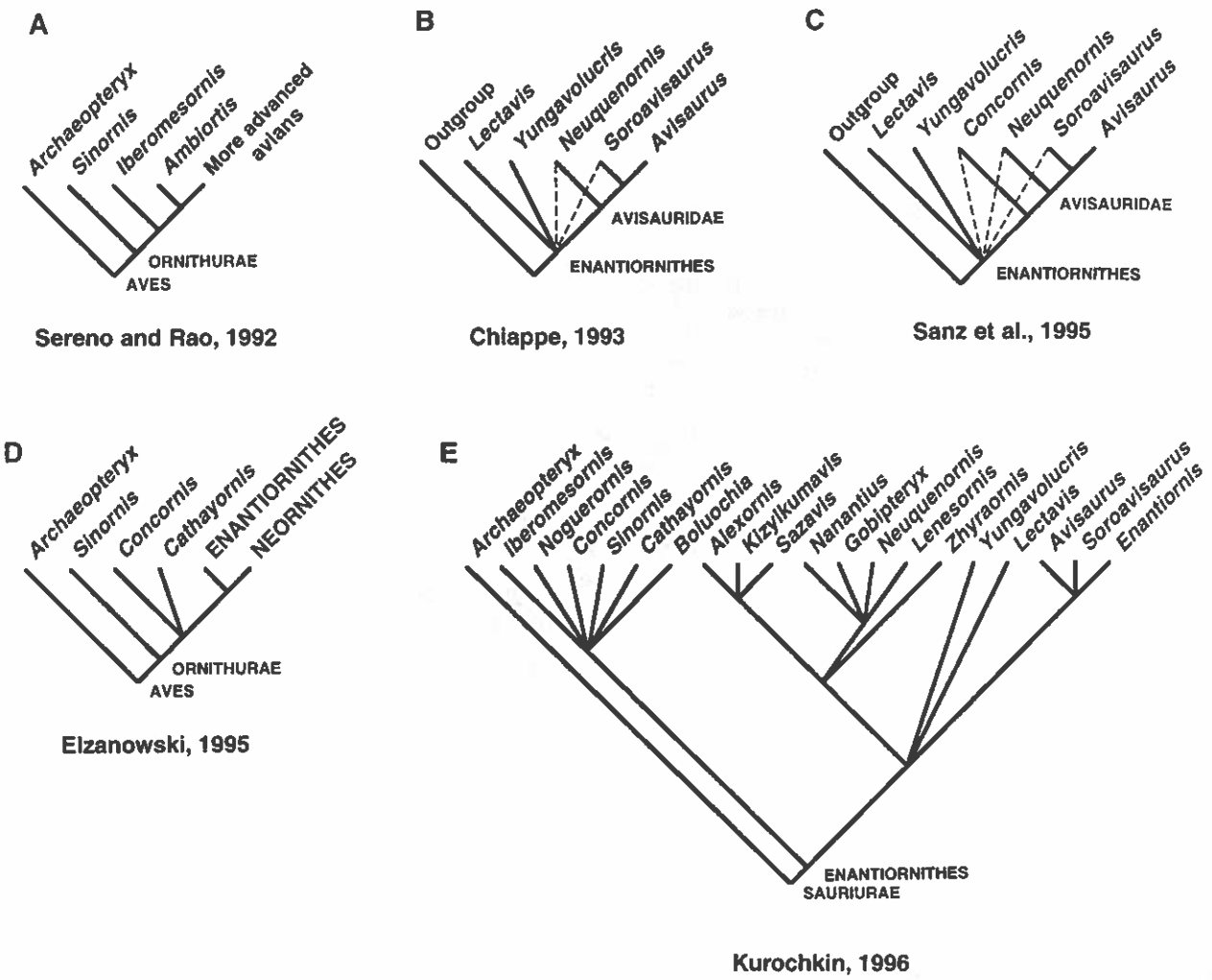

Figure 8.10. Enantiornithine relationships. (A) Phylogeny presented by Sereno and Rao (1992). (B) Relationships proposed by Chiappe (1993), with broken lines showing loss of all resolution for trees one step longer than the minimum. (C) Minimum-length tree presented by Sanz et al. (1995), with broken lines showing loss of all resolution for trees one step longer than the minimum. (D) Phylogenetic diagram presented by Elzanowski (1995). (E) Phylogenetic diagram presented by Kurochkin (1996) showing phylogenetic resolution that is impossible to generate from its associated data matrix.

ture still breaks down with one additional step (13 steps, 13 trees). The tarsometatarsus alone, we conclude, is insufficient to clarify much about higher-level relationships within Enantiornithes.

Elzanowski (1995: Fig. 4) presented a cladogram showing a paraphyletic arrangement of taxa here considered enantiornithines (Fig. 8.10D). Eight synapomorphies were listed to demonstrate that some enantiornithines were more advanced than *Concornis*, *Sinornis*, and *Cathayornis*. As argued previously, *Cathayornis* is a junior synonym of *Sinornis*. The five synapomorphies Elzanowski listed to unite *Concornis*, *Cathayornis*, and other avians to the exclusion of *Sinornis* are flawed, such as the absence of a pubic foot (which is clearly present in the holotypic specimens of *Cathayornis* and *Concornis*), absence of gastralia (also absent in *Sinornis*, as described earlier), and a prominent antitrochanter on the ilium (which is clearly present and prominent in *Sinornis*). The information available to Elzanowski for several of these genera was limited. The holotypic skeletons of *Sinornis* and *Concornis* clearly how many features that establish their inclusion within a monophyletic Enantiornithes (Chiappe, 1991, 1996; Sereno, 2000).

Kurochkin (1996: Fig.13) presented a phylogeny for 19 enantiornithine species (Fig. 8.10E). Although accepting "the principal thesis of a [*sic*] Hennig's taxonomy," Kurochkin (1996:38) suggested that use of parsimony would lead to "an obviously false phylogeny" for basal avians. Per-

haps not surprisingly, his "eclectic" phylogeny bears no discernible relation to an extensive matrix of character data tabulated in the same paper. The matrix includes 122 features scored across 40 terminal entities, which include 27 named taxa, several unnamed specimens, one embryo, and some isolated bones. The data are not a list of characters but rather a mixture of primitive and derived character states, which were then scored, with few exceptions, as present or absent. Missing entries abound; 13 terminal entities are scored for 6 or fewer of the 122 features in the matrix. One terminal unit, an isolated femur, is scored for only one state—the absence of a particular feature. Twenty-four features are constant or otherwise uninformative.

These data give rise to an incalculably enormous number of minimum-length trees of 158 steps. If one omits all terminal units except the outgroups (*Archaeopteryx*, Ichthyornithiformes, Neornithes) and the seven enantiornithines considered by Sanz et al. (1995), 80 features are phylogenetically uninformative. The remainder give rise to 72 minimum-length trees of 51 steps, the strict consensus of which yields a basal polytomy encompassing all included enantiornithines. Although we disagree with many aspects of Kurochkin's data, this result seems to be an accurate gauge of current understanding of enantiornithine phylogeny (see Chiappe and Walker, Chapter 11 in this volume, for additional discussion).

S. santensis, *I. romerali*, *C. lacustris*, and *Eoalulavis hoyasi* are known from well-preserved skeletons of Early Cretaceous age. Their postcranial remains are remarkably uniform and bear few autapomorphies. Reasonably complete cranial remains are known only for *Sinornis*. The Late Cretaceous *Neuquenornis volans* is less complete but also very similar in structure. It is clear, then, that sparrow- to starling-sized enantiornithines with this conservative skeletal design achieved worldwide distribution during the Early Cretaceous. Their interrelationships, nonetheless, are currently unknown. More derived Late Cretaceous enantiornithines include the long-limbed genera *Nanantius* and *Lectavis* and the asymmetrically footed genus *Yungavolucris* (Chiappe, 1993; Kurochkin, 1996). More complete material of these genera may yield character data that will distinguish subgroups within Enantiornithes.

Paleobiology

S. santensis, the most completely known enantiornithine, provides a detailed view of a basal avian that, judging from its skeleton, would have been similar in flight performance and perching capability to sparrow-sized birds living today in arboreal habitats (Fig. 8.8).

The thorax is strengthened to resist forces generated by an increase in pectoral muscle mass. The coracoids expand distally to form broad, lengthened struts to the sternum, which is enlarged and partially keeled. The cranial ribs are particularly robust and are associated with ossified sternal ribs.

The scapula, coracoid, and furcula articulate to form a triosseal canal adjacent to the shoulder joint. Martin (1995) and Ostrom et al. (1999), to the contrary, have stated that a triosseal canal is absent in Enantiornithes. The form of the three bones that would compose the canal, however, suggests otherwise. In enantiornithines the scapula has a long, robust, and craniomedially deflected acromial process; the coracoid, similarly, has a well-developed, dorsally prominent acrocoracoid process; and the furcula has dorsolateral rami that curve laterally and terminate in an expanded articular head (preserved in *Sinornis*, *Concornis*, and *Eoalulavis*). The form of these bones and their configuration as preserved in partial articulation (Sanz et al., 1995: Figs. 6, 7) and in restoration strongly suggest that a triosseal canal of modern avian design was present and would have provided passage for the tendon of the supracoracoideus muscle. The tendon would have inserted on the prominent dorsal tuberosity of the humerus. In enantiornithines, the supracoracoideus muscle with its tendinous attachment to the humerus thus appears to have achieved its modern configuration and function—as an important elevator and, especially, rotator of the wing, functions that are critical for takeoff and landing (Poore et al., 1997; Ostrom et al., 1999). The triosseal canal, in contrast, is not present in either *Archaeopteryx* or *Confuciusornis*.

In the wing, the wrist joint is characterized by a laterally displaced, V-shaped ulnare. Unlike in *Archaeopteryx*, in which the ulnare is positioned distal to the ulna, in enantiornithines and other ornithothoracines the ulnare is displaced lateral to the long axis of the ulna. The V-shaped incisure on the ulnare for the metacarpus allowed greater flexion at the wrist during upstroke, which is important in small-bodied fliers for decreasing drag (Jenkins et al., 1988). At the same time, the enlarged ulnare forms a rigid interlocking wrist joint during downstroke (Vazquez, 1992, 1994).

The first digit of the manus bears alular feathers in the enantiornithine *Eoalulavis* (Sanz et al., 1997). The similar slender form of the first digit in *Sinornis* and other enantiornithines suggests that it also may have borne alular feathers. Alular feathers, which are clearly absent in *Confuciusornis* and *Archaeopteryx*, help to prevent turbulent airflow over the wing, enhancing maneuverability at slow speeds.

Several features in the pes suggest that *Sinornis* and other well-known enantiornithines (e.g., *Neuquenornis*, *Concornis*, *Iberomesornis*) had achieved advanced perching function and lived primarily in an arboreal habitat. Advanced perching function is indicated by the presence of a fully opposable hallux with a particularly large ungual (Sereno and Rao, 1992). In *Sinornis* the three principal digits of the pes are long compared with the tibia or femur, the penultimate pedal phalanges are lengthened, and the pedal claws are

strongly recurved (Peters and Görgner, 1992; Feduccia, 1993). The lengthening of the penultimate phalanges of the pedal digits is probably the best single indicator of habitat preference (Hopson and Chiappe, 1998; Hopson, 2001).

Conclusions

We have drawn the following conclusions based on our study of *S. santensis* and other basal avians:

1. *C. yandica* is a junior synonym of *S. santensis.*
2. *S. santensis* is currently the most completely known enantiornithine and is very close in skeletal form and body size to *I. romerali, C. lacustris,* and *E. hoyasi.*
3. Enantiornithes, defined as all ornithothoracines more closely related to *Sinornis* than to Neornithes, is a monophyletic clade united by many skeletal features.
4. Phylogenetic relationships among enantiornithines remain poorly established, because several genera (*Sinornis, Iberomesornis, Concornis, Eoalulavis, Neuquenornis*) differ in only minor ways and because taxa with more derived features (*Nanantius, Lectavis, Yungavolucris, Avisaurus, Soroavisaurus*) are, to date, very incomplete.
5. The increase in robustness of the ribcage and sternum, a triosseal canal, the advanced design of the wrist bones, the presence of alular feathers, and the design of the pes suggest that *Sinornis* and other similar-sized enantiornithines were arboreal birds that had achieved a level of performance in flight and perching that would be indistinguishable from sparrow-sized birds living today.

Acknowledgments

We thank C. Abraczinskas for execution of the camera lucida drawings and matching labeled figures. We also thank J. L. Sanz, A. D. Buscalioni, L. M. Chiappe, L. D. Martin, L. M. Witmer, and Zhou Z. for discussing aspects of anatomy and for access to specimens in their care.

Literature Cited

Barrett, P. M. 2000. Evolutionary consequences of dating the Yixian Formation. Trends in Ecology and Evolution 15:99–103.

Chatterjee, S. 1995. The Triassic bird *Protoavis. Archaeopteryx* 13:15–31.

Chen P. 1988. Distribution and migration of Jehol fauna with reference to nonmarine Jurassic-Cretaceous boundary in China. Acta Palaeontologica Sinica 27:681–683.

Chiappe, L. M. 1991. Cretaceous avian remains from Patagonia shed new light on the early radiation of birds. Alcheringa 15:333–338.

———. 1992. Enantiornithine (Aves) tarsometatarsi and the avian affinities of the Late Cretaceous Avisauridae. Journal of Vertebrate Paleontology 12:344–350.

———. 1993. Enantiornithine (Aves) tarsometatarsi from the Cretaceous Lecho Formation of northwestern Argentina. American Museum Novitates 3083:1–27.

———. 1995. The first 85 million years of avian evolution. Nature 378:349–355.

———. 1996. Late Cretaceous birds of southern South America: anatomy and systematics of Enantiornithes and *Patagopteryx deferrariisi;* pp. 203–244 *in* G. Arratia (ed.), Contributions of Southern South America to Vertebrate Paleontology, Münchner Geowissenschaftliche Abhandlungen, Reihe A, Geologie und Paläontologie 30. Verlag Dr. Friedrich Pfeil, Munich.

Chiappe, L. M., and J. O. Calvo. 1994. *Neuquenornis volans,* a new Late Cretaceous bird (Enantiornithes: Avisauridae) from Patagonia, Argentina. Journal of Vertebrate Paleontology 14:230–246.

Chiappe, L. M., M. A. Norell, and J. M. Clark. 1996. Phylogenetic position of *Mononykus* (Aves: Alvarezsauridae) from the Late Cretaceous of the Gobi Desert. Memoirs of the Queensland Museum 39:557–582.

———. 1998. The skull of a relative of the stem-group bird *Mononykus.* Nature 392:275–278.

Chiappe, L. M., Ji S., Ji Q., and M. A. Norell. 1999. Anatomy and systematics of the Confuciusornithidae (Theropoda:Aves) from the Late Mesozoic of northeastern China. Bulletin of the American Museum of Natural History 242:1–89.

Cracraft, J. 1986. The origin and early diversification of birds. Paleobiology 12:383–399.

Dementjev, G. P. 1940. Handbook on Zoology. Volume 6, Vertebrates. Birds. Academy of Sciences, Moscow-Leningrad, 856 pp. [Russian].

Elzanowski, A. 1995. Cretaceous birds and avian phylogeny. Courier Forschungsinstitut Senckenberg 181:37–53.

Elzanowski, A., and P. Wellnhofer. 1996. Cranial morphology of *Archaeopteryx:* evidence from the seventh skeleton. Journal of Vertebrate Paleontology 16:81–94.

Feduccia, A. 1993. Evidence from claw geometry indicating arboreal habits of *Archaeopteryx.* Science 259:790–793.

Forster, C. A., S. D. Sampson, L. M. Chiappe, and D. W. Krause. 1998. The theropod ancestry of birds: new evidence from the Late Cretaceous of Madagascar. Science 279:1915–1919.

Gauthier, J. 1986. Saurischian monophyly and the origin of birds; pp. 1–55 *in* K. Padian (ed.), The Origin of Birds and the Evolution of Flight. California Academy of Sciences, San Francisco.

Hong Y. 1988. Early Cretaceous Orthoptera, Neuroptera, Hymenoptera (Insecta) of Kezuo in west Liaoning Province. Entomotaxonomia 10:128–130.

Hopson, J. A. 2001. Ecomorphology of avian and nonavian theropod phalangeal proportions: implications for the arboreal versus terrestrial origin of bird flight; pp. 211–235 *in* J. Gauthier and L. F. Gall (eds.), New Perspectives on the Origin and Early Evolution of Birds: Proceedings of the International Symposium in Honor of John H. Ostrom. Peabody Museum of Natural History, New Haven.

Hopson, J. A., and L. M. Chiappe. 1998. Pedal proportions of living and fossil birds indicate arboreal or terrestrial specialization. Journal of Vertebrate Paleontology 18:52A.

Hou L. 1997. Mesozoic Birds of China. Taiwan Provincial Feng Huang Ku Bird Park, Nan Tou, Taiwan, 228 pp.

Hou L., Zhou Z., L. D. Martin, and A. Feduccia. 1995. A beaked bird from the Jurassic of China. Nature 377:616–618.

Hou L., L. D. Martin, Zhou Z., and A. Feduccia. 1996. Early adaptive radiation of birds: evidence from fossils from northeastern China. Science 274:1164–1167.

Jenkins, F. A., Jr., K. P. Dial, and G. E. Goslow Jr. 1988. A cineradiographic analysis of bird flight: the wishbone in starlings is a spring. Science 241:1495–1498.

Ji Q., Ji S., Ren D., Lu L., Fang X., and Gou Z. 1999. On the sequence and age of the proto-bird bearing deposits in the Sihetun-Jianshangou area, Beipiao, western Liaoning. Professional Papers in Stratigraphy and Paleontology 27:75–80. [Chinese]

Kurochkin, E. N. 1985. A true carinate bird from Lower Cretaceous deposits in Mongolia and other evidence of Early Cretaceous birds in Asia. Cretaceous Research 6:271–278.

———. 1996. A New Enantiornithid of the Mongolian Late Cretaceous, and a General Appraisal of the Infraclass Enantiornithes (Aves). Palaeontological Institute, Moscow, 60 pp.

Marsh, O. C. 1880. Odontornithes: A Monograph on the Extinct Toothed Birds of North America. Report of Geological Exploration of the 40th Parallel. Government Printing Office, Washington, D.C., 201 pp.

Martin, L. D. 1983. The origin and early radiation of birds; pp. 291–338 *in* A. H. Bush and G. A. Clark Jr. (eds.), Perspectives in Ornithology. Cambridge University Press, Cambridge.

———. 1995. The Enantiornithes: terrestrial birds of the Cretaceous. Courier Forschungsinstitut Senckenberg 181:23–36.

Martin, L. D., Zhou Z., Hou L., and A. Feduccia. 1998. *Confuciusornis sanctus* compared to *Archaeopteryx lithographica.* Naturwissenschaften 85:286–289.

Molnar, R. E. 1986. An enantiornithine bird from the Lower Cretaceous of Queensland, Australia. Nature 322:736–738.

Norell, M. A., and P. J. Makovicky. 1997. Important features of the dromaeosaur skeleton: information from a new specimen. American Museum Novitates 3215:1–28.

Novas, F. E. 1997. Anatomy of *Patagonykus puertai* (Theropoda, Maniraptora, Alvarezsauridae) from the Late Cretaceous of Patagonia. Journal of Vertebrate Paleontology 17:137–166.

Ostrom, J. H., S. O. Poore, and G. E. Goslow Jr. 1999. Humeral rotation and wrist supination: important functional complex for the evolution of powered flight in birds?; pp. 301–309 *in* S. L. Olson (ed.), Paleontology at the Close of the 20th Century: Proceedings of the 4th International Meeting of the Society of Avian Paleonotology and Evolution, Washington, D.C., 4–7 June 1996. Smithsonian Contributions to Paleobiology 89. Smithsonian Institution Press, Washington.

Padian, K., and L. M. Chiappe. 1998. The origin and early evolution of birds. Biological Reviews 73:1–42.

Peters, D. S., and E. Görgner. 1992. A comparative study on the claws of *Archaeopteryx;* pp. 29–37 *in* K. E. Campbell Jr. (ed.), Papers in Avian Paleontology, Honoring Pierce Brodkorb. Science Series 36. Natural History Museum of Los Angeles County, Los Angeles.

Poore, S. O., A. Sanchéz-Haiman, and G. E. Goslow Jr. 1997. Wing upstroke and the evolution of flapping flight. Nature 387: 799–802.

Rao C. and P. C. Sereno. 1990. Early evolution of the avian skeleton: new evidence from the Lower Cretaceous of China. Journal of Vertebrate Paleontology 10:38–39A.

Sanz, J. L., and J. F. Bonaparte. 1992. A new order of birds (Class Aves) from the Lower Cretaceous of Spain; pp. 39–49 *in* K. E. Campbell Jr. (ed.), Papers in Avian Paleontology, Honoring Pierce Brodkorb. Science Series 36. Natural History Museum of Los Angeles County, Los Angeles.

Sanz, J. L., and A. D. Buscalioni. 1992. A new bird from the Early Cretaceous of Las Hoyas, Spain, and the early radiation of birds. Palaeontology 35:829–845.

Sanz, J. L., J. F. Bonaparte, and A. Lacasa. 1988. Unusual Early Cretaceous birds from Spain. Nature 331:433–435.

Sanz, J. L., L. M. Chiappe, and A. D. Buscalioni. 1995. The osteology of *Concornis lacustris* (Aves: Enantiornithes) from the Lower Cretaceous of Spain and a reexamination of its phylogenetic relationships. American Museum Novitates 3133:1–23.

Sanz, J. L., L. M. Chiappe, B. P. Pérez-Moreno, A. D. Buscalioni, J. J. Moratalla, F. Ortega, and F. J. Poyato-Ariza. 1996. An Early Cretaceous bird from Spain and its implications for the evolution of avian flight. Nature 382:442–445.

Sanz, J. L., L. M. Chiappe, B. P. Pérez-Moreno, J. Moratalla, F. Hernández-Carrasquilla, A. D. Buscalioni, F. Ortega, F. J. Poyato-Ariza, D. Rasskin-Gutman, and X. Martínez-Delclòs. 1997. A nestling bird from the Lower Cretaceous of Spain: implications for avian neck and skull evolution. Science 276: 1543–1546.

Sereno, P. C. 1997. The origin and evolution of dinosaurs. Annual Review of Earth and Planetary Science 25:435–489.

———. 1998. A rationale for phylogenetic definitions, with application to the higher-level taxonomy of Dinosauria. Neues Jahrbuch für Geologie und Paläontologie 210:41–83.

———. 1999a. The evolution of dinosaurs. Science 284:2137–2147.

———. 1999b. Definitions in phylogenetic taxonomy: critique and rationale. Systematic Biology 48:329–351.

———. 1999c. A rationale for dinosaurian taxonomy. Journal of Vertebrate Paleontology 19:788–790.

———. 2000. *Iberomesornis romerali* (Aves, Ornithothoraces) reevaluated as an Early Cretaceous enantiornithine. Neues Jarhbuch für Geologie und Paläontologie Abhandlungen 215:365–395.

———. 2001. Alvarezsauridae (Dinosauria, Coelurosauria): birds or ornithomimosaurs?; pp. 69–98 *in* J. Gauthier and L. F. Gall (eds.), New Perspectives on the Origin and Early Evolution of Birds: Proceedings of the International Symposium in Honor of John H. Ostrom. Peabody Museum of Natural History, New Haven.

Sereno, P. C., and Rao C. 1992. Early evolution of avian flight and perching: new evidence from the Lower Cretaceous of China. Science 55:845–848.

Sereno, P. C., Chao S., Cheng Z., and Rao C. 1988. *Psittacosaurus meileyingensis* (Ornithischia: Ceratopsia), a new psittacosaur from the Lower Cretaceous of northeastern China. Journal of Vertebrate Paleontology 4:366–377.

Swisher, C. C., III, Wang Y.-Q., Wang X.-L., Xu X., and Wang Y. 1999. Cretaceous age for the feathered dinosaurs of Liaoning, China. Nature 400:58–61.

Vazquez, R. J. 1992. *Archaeopteryx* and powered flight. Research and Exploration 8:387–388.

———. 1994. The automating skeletal and muscular mechanisms of the avian wing (Aves). Zoomorphology 114:59–71.

Walker, C. A. 1981. A new subclass of birds from the Cretaceous of South America. Nature 292:51–53.

Wang X.-L., Wang Y.-Q., Xu X., Tang Z., Zhang F., and Hu Y. 1998. Stratigraphic sequence and vertebrate-bearing beds of the lower part of the Yixian Formation in Sihetun and neighboring area, western Liaoning, China. Vertebrata PalAsiatica 36:96–101.

Wellnhofer, P. 1974. Das fünfte Skelettexemplar von *Archaeopteryx*. Palaeontographica Abhandlungen A 147:169–216.

Zhou Z. 1995a. Discovery of a new enantiornithine bird from the Early Cretaceous of Liaoning, China. Vertebrata PalAsiatica 1994:99–113.

———. 1995b. The discovery of Early Cretaceous birds in China. Courier Forschungsinstitut Senckenberg 181:9–22.

Zhou Z., Fan F. J., and Zhang J. 1992. Preliminary report on a Mesozoic bird from Liaoning, China. Chinese Science Bulletin 37:1365–1368.